

TUNING THE HARDNESS AND WETTABILITY OF METHACRYLATE
POLYMERS

TUNING THE HARDNESS AND WETTABILITY OF METHACRYLATE
POLYMERS

By NICHOLAS LUONG, B.SC. HONS.

A Thesis Submitted to the School of Graduate Studies in Partial Fulfilment of the
Requirements for the Degree Master of Science

McMaster University © Copyright by Nicholas Luong, September 2012

McMaster University MASTER OF SCIENCE (2012) Hamilton, Ontario (Chemistry)

TITLE: Tuning the Hardness and Wettability of Methacrylate Polymers

AUTHOR: Nicholas Luong, B.Sc. Hons. (York University)

SUPERVISOR: Professor Michael A. Brook NUMBER OF PAGES: ix, 71

Abstract

Silicones exhibit a fundamentally hydrophobic character. While the incorporation of hydrophilic surface moieties can be achieved by a variety of means, normally surface reversion leads to rapid recovery of hydrophobic surfaces. We were interested to learn if the hydrophobic character of silicones could be manifested on organic polymers and, moreover, if different degrees of wetting of organic surfaces could be controlled by simultaneous use of more than one hydrophilic entity.

Herein, we present a method to control the hardness and wettability of methacrylate polymers with the addition of ACR A008-UP, a polymerizable, acrylate-based trisiloxane surfactant. Surface wettabilities were determined through the use of contact angle measurements, and the hardness modulus is determined through the use of a Shore OO durometer. The wettability and the hardness of the polymers were controlled by varying the ratio of surfactant to methacrylate monomers. As the proportion of surfactant monomer increased, the hardness of the copolymers was depressed. In a similar fashion, as the proportion of surfactant increased, the copolymer surfaces became increasingly wettable. However, at a certain threshold concentration the wettability decreased once again, which is ascribed to the formation of a hydrophobic brush at higher concentrations. The wettability and hardness of the polymers, and the stability of the trisiloxanes on the surface will be discussed.

Acknowledgements

First and foremost, I would like to thank Dr. Michael A. Brook. Without his unwavering support, frequent advice, and humorous personality, the completion of this work would not have been possible. Not only is he a great mentor and teacher, he is also a good friend and fellow chorister.

Thank you to all members of the current Brook group, in particular: Beth Laidley, Laura Dodge, Madiha Khan, and Mark Pascoal for keeping me company all these years.

I would also like to thank Jason Jianfeng Zhang. He has always been there when I am in need of someone to complain to, confide in, or to plainly converse with. A lot of things would not have been possible if it wasn't for his friendship and help.

From within the McMaster community, I would like to thank Iris Kwok and Janice Cheung. Without your emotional support and enthusiasm, these 2 years would have been very difficult.

Lastly, nothing would have been possible without the love of my parents, siblings, and girlfriend, Samantha. I thank you all and I love you all dearly too.

Table Contents

1. Introduction.....	1
1.1. Contact Lenses	1
1.2. Bioapplications of methyl methacrylate polymers	4
1.3. Trisiloxane ethoxylate surfactants	4
1.4. Trisiloxane Surfactant Adjuvants in Pesticides	9
1.5. Contact Angle	9
1.6. Hardness of Polymers	11
2. Proposal	13
3. Results and Discussion	15
3.1. Synthesis of Polymers.....	15
3.2. Polymer Characterization	15
3.3. Spontaneous Surface Structures.....	16
3.4. Hardness of ACR-MMA-BMA Polymers	19
3.5. Extractions of ACR-MMA-BMA Polymers.....	24
3.6. Wettability of ACR-MMA-BMA Polymers	29
3.7. Stability of the ACR-MMA-BMA Polymer Surface	38
3.8. Controlling Surface Properties of Biomaterials.....	40
4. Conclusion	43
5. Materials and Methods	44
5.1. Chemicals.....	44
5.2. Polymer Synthesis.....	44
5.3. Synthesis of ACR-MMA-BMA Polymers.....	45
5.4. Synthesis of hPEG-MMA-BMA Polymers	49
5.5. Synthesis of oPEG	49
5.6. Synthesis of oPEG-MMA-BMA Polymers	52
5.7. Shore Hardness Measurements.....	52
5.8. Wettability Measurements	52
5.9. Trisiloxane Stability Study	53

5.10. Soxhlet Extraction.....	53
5.11. Surface Analysis	53
5.12. Chemical Structure Analysis	54
5.13. Mass Determination.....	54
6. References.....	55
7. Appendix.....	62
7.1. E. coli GFP Fluorescence.....	62
7.2. NMR Spectra of Select ACR-methacrylate Polymers	63
7.2.1. 40-00-60.....	63
7.2.2. 40-30-30.....	64
7.2.3. 40-60-00.....	65
7.2.4. 60-00-40.....	66
7.2.5. 60-20-20.....	67
7.2.6. 60-40-00.....	68
7.2.7. 80-00-20.....	69
7.2.8. 80-10-10.....	70
7.2.9. 80-20-00.....	71

List of Figures

Figure 1:	The general structure of trisiloxane ethoxylate surfactants.....	5
Figure 2:	An aqueous solution with trisiloxane surfactants spreading on surfaces with different energies.....	8
Figure 3:	Shapes of water droplets placed on non-absorbent surfaces.....	10
Figure 4:	The chemical structures of the monomers and crosslinker.....	14
Figure 5:	Scanning electron microscopy images of spontaneous surface structures.....	18
Figure 6:	Differences in light penetration of polymer body.....	19
Figure 7:	The chemical structure of a poly(acrylic) and poly(methacrylic) homopolymer.....	20
Figure 8:	The Shore OO hardness of ACR-methacrylate polymers.....	23
Figure 9:	Percent weight loss after subsequent extractions.....	25
Figure 10:	The nuclear magnetic resonance spectrum of the extracted material.....	26
Figure 11:	The nuclear magnetic resonance spectrum of the ACR monomer.....	27
Figure 12:	The nuclear magnetic resonance spectrum of methyl methacrylate.....	28
Figure 13:	The wettability of ACR-methacrylate polymers.....	33
Figure 14:	The wettability of hPEG-methacrylate copolymers.....	34
Figure 15:	The wettability of oPEG-methacrylate polymers.....	34
Figure 16:	Oleate-PEG clusters adsorbed to elastomer surface.....	35
Figure 17:	A proposal for the unusual wettability of ACR-methacrylate polymers.....	36
Figure 18:	The progression of the mushroom to the brush regime as a function of increasing graft density.....	37
Figure 19:	The wettability of selected ACR-methacrylate polymers over a three week period.....	39
Figure 20:	The mass spectrum of oPEG.....	50
Figure 21:	The nuclear magnetic spectrum of the oPEG monomer.....	51

List of Tables

Table 1:	Glass Transition Temperatures for Selected Poly(methacrylic) Homopolymers (R = Me, Figure 7)	21
Table 2:	Formulation for ACR-MMA-BMA Polymers	46
Table 3:	Ratio of Monomers Incorporated into Oligomers of the Extracted Material..	47
Table 4:	Ratio of Monomers Incorporated into Polymers.....	48
Table 5:	Formulation for hPEG-MMA-BMA Polymers	49
Table 6:	Formulation for oPEG-MMA-BMA Polymers	52

List of Abbreviations and Symbols

ACR	ACR A008-UP surfactant monomer
EDB	Ethyl 4-(dimethylamino)benzoate
BMA	Butyl methacrylate
CQ	Camphorquinone
DEGDA	Diethylene glycol diacrylate
HEMA	2-Hydroxyethyl methacrylate
HMDZ	Hexamethyldisilazane
hPEG	Hydroxy-PEG-acrylate monomer
oPEG	Oleate-PEG-acrylate monomer
MEHQ	Hydroquinone monomethyl ether
MMA	Methyl methacrylate
NMR	Nuclear magnetic resonance spectroscopy
NRK	Normal rat kidney
PAA	Poly(acrylic acid)
PACR	Poly(ACR)
PBMA	Poly(butyl methacrylate)
PDMS	Poly(dimethylsiloxane)
PEG	Poly(ethylene glycol)
PhPEG	Poly(hPEG)
PHEMA	Poly(2-hydroxyethyl methacrylate)
PMMA	Poly(methyl methacrylate)
PoPEG	Poly(oPEG)
PSA	Pressure sensitive adhesive
PU	Poly(urethane)
SEM	Scanning electron microscopy
T_g	Glass transition temperature

1. Introduction

1.1. Contact Lenses

The eye is a very sensitive and complex organ in the human body, and maintaining its health and functionality is important. Contact lenses provide temporary vision correction by altering incoming light rays resulting in a shift of the focal point of the image in the eye. Since the cornea of the eye requires an adequate supply of oxygen to maintain its health, its accessibility to oxygen will be effectively changed when contact lenses are placed upon it; the atmosphere is the primary source of oxygen for the cornea. Ideal contact lenses should not only be comfortable for the wearer, but also be able to maintain a continuous tear film, inert to the components in the tear, maintain hydration, and be permeable to oxygen and ions (*1*).

In 1930s, the first commercial contact lenses, made of poly(methyl methacrylate) (PMMA), were created (*2*); however, they had a major drawback of being uncomfortable, lacking permeability to oxygen, and can shatter, as PMMA is a hard organic glass. In 1960, Wichterle introduced first soft lenses created from a hydrogel of poly(2-hydroxyethyl methacrylate) (HEMA), and this revolutionized contact lens research (*3*). DeCarle, in the 1970s, experimented with extended wear contact lenses; however, problems soon arose due to corneal oxygen deprivation (*4,5*).

Silicones have good oxygen permeability due to the bulkiness of the methyl group on the siloxane backbone – which prevents adjacent chains from approaching too closely, leaving a high free volume – and the mobility of the polysiloxane polymers, which results from the very large Si-O-Si linkage (about 145°). In 1980, Dow Corning developed

Elastofilcon A, the first soft silicone contact lens, but issues arose from its lack of wettability (*1*). These lens were hydrophobic, rubbery, and could adhere to the cornea; therefore, they are only used as lens replacements for people with aphakia (*1*). Research continued to try and find ways to create silicone lenses that were also highly wettable to facilitate comfort and eliminate adhesion to the cornea. As a consequence, modern day contact lenses are generally ABA block copolymers of siloxanes and a hydrophilic monomer like 2-hydroxyethyl methacrylate (HEMA); the silicones allow for oxygen permeability and PHEMA for wettability (*1*). Aside from HEMA, poly(*N*-vinylpyrrolidone) and poly(dimethylacrylamide) can also be used as the hydrophilic monomers to bring wettability to hydrophobic silicone polymers (*1*). However, not only hydrophilic monomers are incorporated into silicones. Hydrophobic monomers can also be used so that physical properties like mechanical strength, final refractive index, and wettability can be tuned (*1*). Hydrophobic monomers commonly used are aliphatic esters of acrylic and methacrylic acid.

Aside from the wettability of contact lenses, the hardness (modulus) of the lenses must also be considered, as the literature reports variances in cell adhesion to surfaces of different hardness (*6*); the adhesion of cells and bacteria to the contact lens may foul the polymer, and can potentially lead to secondary medical conditions.

Most normal tissue cells are anchorage dependent and will not thrive in solution, even if all the necessary biomolecules are available (*7,8*). The substrate to which cells adhere can vary in hardness from glass to soft tissues (*7*). In a study by Pelham et al., they indirectly monitored the formation of the cytoskeleton by observing the distribution of

rhodamine-labelled vinculin inside normal rat kidney (NRK) cells on surfaces of different hardness moduli (9). In the cells on harder substrates, the imaged vinculin appears as long fibres, indicating incorporation into the normal development of the cytoskeleton; however, on softer substrates, cells appear as small and irregular shapes. Comparison of these two different phenotypes show there is a difference in the cytoskeletal development, which indicates a difference in adhesion and even mobility of the cells. Pelham et al. proposed two hypotheses to help explain how cells sense substrate hardness. The first hypothesis involves cells pushing and pulling the integrin receptors. These receptors are found on the cell membrane and attached to the cytoskeleton and, depending how the surface responds, different signalling pathways will be (de)activated via changes in tyrosine phosphorylation. The second hypothesis involves the activation of force-sensitive enzyme complexes that are coupled to the integrin receptors via the cytoskeleton. Dependent on adhesion to the surface, the forces exerted on the adhesion complexes will activate the force-sensitive enzymes leading to downstream signalling (9).

A recent study by Lichter et al. examined how substrate hardness affects the adhesion of *Staphylococcus epidermis* and *Escherichia coli* on weak polyelectrolyte multilayer thin films (10). In a layer by layer dipcoat deposition method onto medical grade titanium, they created surfaces with varying elastic moduli between 1 MPa and 100 MPa. By changing the thickness of the polyelectrolyte coating of poly(methacrylic acid) and poly(allylamine hydrochloride), it was possible to correlate surface hardness with bacterial adhesion. On the harder uncoated titanium surface, there were significantly more

viable bacterial colonies than on the softer polyelectrolyte coated surfaces; bacteria preferentially adhere to harder surfaces than softer ones.

1.2. Bioapplications of methyl methacrylate polymers

Recent literature reports have examined the viability of a variety of synthetic polymers that hold potential as materials for biomedical applications (*11,12,13*). One important material continues to be the polymer poly(methyl methacrylate) (PMMA), which is found in rigid contact lenses, intraocular lenses, acrylic cements, and fillings for bone cavities (*13*). PMMA is hydrophobic, which may not be optimal for use in various biological environments. Different synthetic polymers will exhibit varying degrees of surface wettability due to their unique chemical compositions on the surface. As a consequence, the literature also reports that the hydrophilization of a polymer surface will lower non-specific protein adsorption (*14,15*), and reduce the adhesion of bacteria (*16*) and cells (*15*) to the polymer that, in the best cases, can reduce the foreign body response (*17*). There is interest, therefore, in developing methods that permit control over the hydrophilicity of biomaterials surfaces.

1.3. Trisiloxane ethoxylate surfactants

Trisiloxane surfactants are amphiphilic molecules comprised of a trisiloxane hydrophobe linked to a hydrophilic oligo(ethylene glycol) chain via an alkyl spacer (Figure 1).

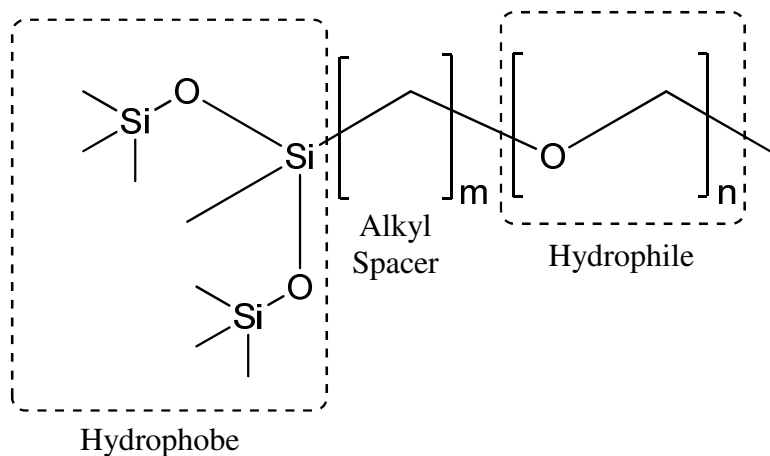


Figure 1: The typical structure of trisiloxane ethoxylate surfactants ($m > 0$; $n > 0$). They generally consists of an oligo(ethylene glycol) hydrophile linked to a small silicone hydrophobe via an alkyl spacer.

When small amounts of trisiloxane surfactants are added to an aqueous solution (e.g., 0.1% w/w), the rapid spreading of the solution across hydrophobic surfaces like Parafilm™, and sheets of poly(ethylene) and poly(propylene), is promoted (18,19). For example, a 50 μ L drop of aqueous solution containing only 0.1 % w/w trisiloxane surfactants will spread, on a polypropylene sheet, up to 8 cm in diameter in 10 seconds, which is approximately 20 times the surface area coverage of an aqueous solution containing the efficient surfactant 1 % w/w nonylphenol ethoxylate (19). Similar droplet dynamics were reported by Halverson et al. when a sessile drop of solution of trisiloxane-doped aqueous solution was allowed to spread – over only 3 seconds – to a thin film on a polycarbonate surface (20). Compared to conventional surfactants, therefore, these trisiloxane surfactants are superior at facilitating the rapid spreading of an aqueous solution over hydrophobic surfaces. This remarkable property of trisiloxane surfactants led them to be referred to as *superwetters* (18).

Various researchers have looked at the wetting properties of the surfactant as a function of the hydrophobe size, the length of the hydrophilic poly(ethylene glycol) (PEG) chain, temperature, and concentration of the surfactant in the solution. Kanner et al. observed that a surfactant with 2 to 5 silicon atoms exhibits the greatest wetting ability (21). The rate of spreading and the final area of coverage of water droplets can also be controlled by the number of repeating PEG units in the surfactant. Surfactants with 6 repeating PEG units were found to exhibit greater rates and areas of coverage than analogous species with less than or greater than 6 repeating units (22). An increase in the number of PEG units was associated with a decreased surfactant ability to spread across hydrophobic surfaces (23). Surfactants with 6 repeating units also showed the greatest spreading at room temperature; spreading is reduced at higher and lower temperatures (24). Zhu et al. reported that the rate of spreading and the extent of the coverage is proportional to the concentration of the surfactant in the solution; the area of coverage will continue to increase in size, linearly with time, until all the surfactant molecules have migrated to the liquid-air and liquid-surface interfaces (25).

Surfactant molecules dissolved in an aqueous medium can self-assemble into structures. Within a solution, they can potentially form micelles or vesicles, and at the interfaces, they are able to assemble into monolayers or bilayers (26). In a detailed analysis by Tiberg et al., which focused on the surfactant molecules at the interfaces, it was reported that the bulk orientation of the surfactant molecules in an aqueous solution will vary depending on the nature of the surface on which it is spreading (27). On low energy surfaces like hexamethyldisilazane (HMDZ)-modified silicon wafers, the

hydrophobes of the surfactant molecules in an aqueous solution will migrate to the liquid-air and liquid-surface interface forming a monolayer around the entire droplet. On high energy surfaces like silica, by contrast, the surfactant molecules in water will migrate to the liquid-air but not the liquid-surface interface. For surfaces whose energy levels are intermediate, majority of the surfactant molecules will be located as a monolayer at the liquid-air interface, while some are located at the liquid-surface interface, and this leads to the formation of shoulders (Figure 2) (27). This formation of a second front is supported by the observations of Karapetsas et al. (26).

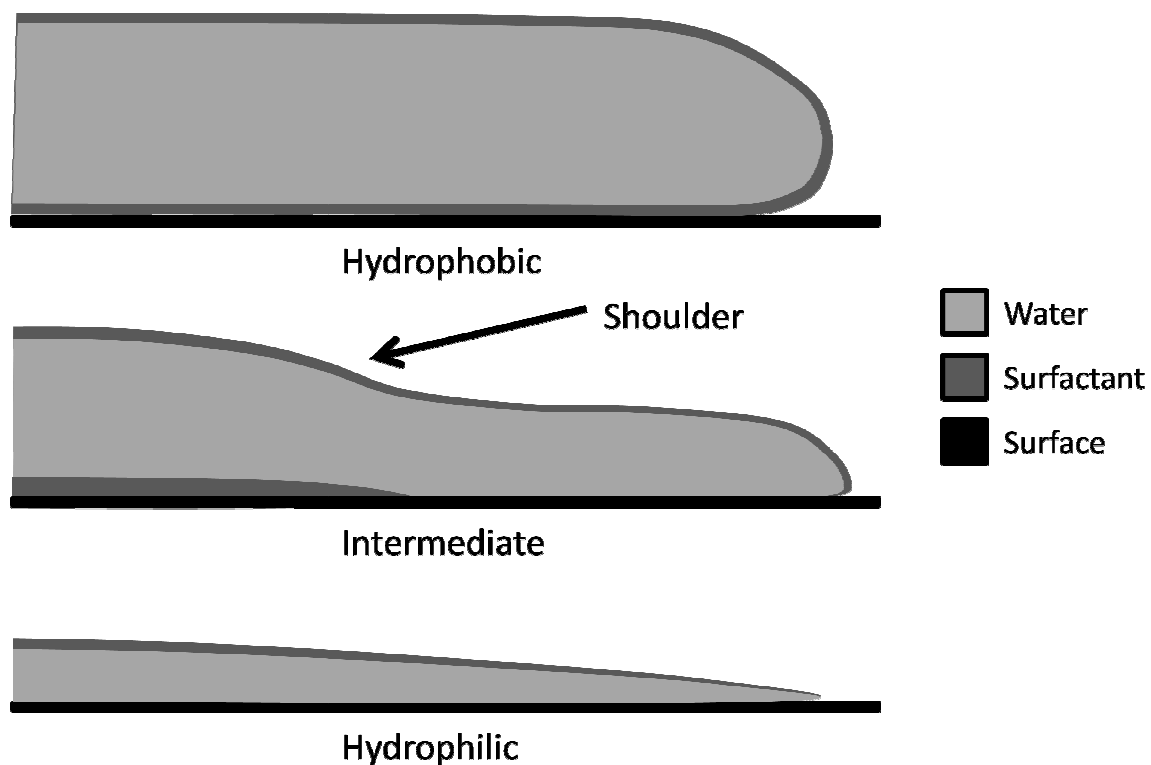


Figure 2: An aqueous solution with trisiloxane surfactants spreading on surfaces with different energies.

Several researchers propose that the enhanced wetting by trisiloxane surfactants, when compared to purely organic surfactants, is due to the Marangoni effect. However, they also believe that it is not the sole effect that governs the rapid wetting ability (26). For example, Rafai et al. attribute the rapid rate of wetting to the surfactant's affinity for the surface (28), while Kumar et al. attributes it to the rapid adsorption of micelles to the liquid-air and liquid-surface interface (29). The molecular dynamic study presented by Karapetsas et al. supports the idea of mono- and bilayer surfactant structures unzipping into the interface monolayers (26). This rapid adsorption of surfactant molecules into the interfacial monolayers can help explain the rapid spreading of the droplet on the surface.

Irrespective of the origin of the wetting ability, the surfactants are useful in a variety of applications.

1.4. Trisiloxane Surfactant Adjuvants in Pesticides

Surfactant adjuvants are used as wetting agents in pesticides. Non-ionic surfactants used for such applications include alcohol ethoxylates, alkylphenol ethoxylate, and trisiloxane ethoxylates (30). By decreasing the surface tension of the aqueous solution, the even distribution of the pesticide across foliar surfaces, in particular, waxy leaf surfaces is facilitated. An increase in the area of coverage by the pesticide also increases the foliar uptake of the pesticide by the plant resulting in a more effective application (19,31,32,33). In addition, by allowing the solution to spread and not collect on the foliar surfaces, the possibilities of chemical burns to the leaf surface is lowered. In essence, the surfactant operates to moderate the delivery of the active ingredient.

1.5. Contact Angle

When an aqueous droplet is placed onto a non-absorbent surface, it will sit on the surface exhibiting the shape of a truncated sphere (Figure 3). The contact angle is measured through the water phase at the triple contact point; an equilibrium occurs where the interfacial tensions between all three phases are balanced. Young developed an equation to describe this relationship in the early 1800s known as Young's equation (34). More recently, Tadmore reported that by using the maximal advancing and minimal receding contact angles, the Young's equilibrium contact angle can also be derived as long the droplet volume and interfacial energies are known (35).

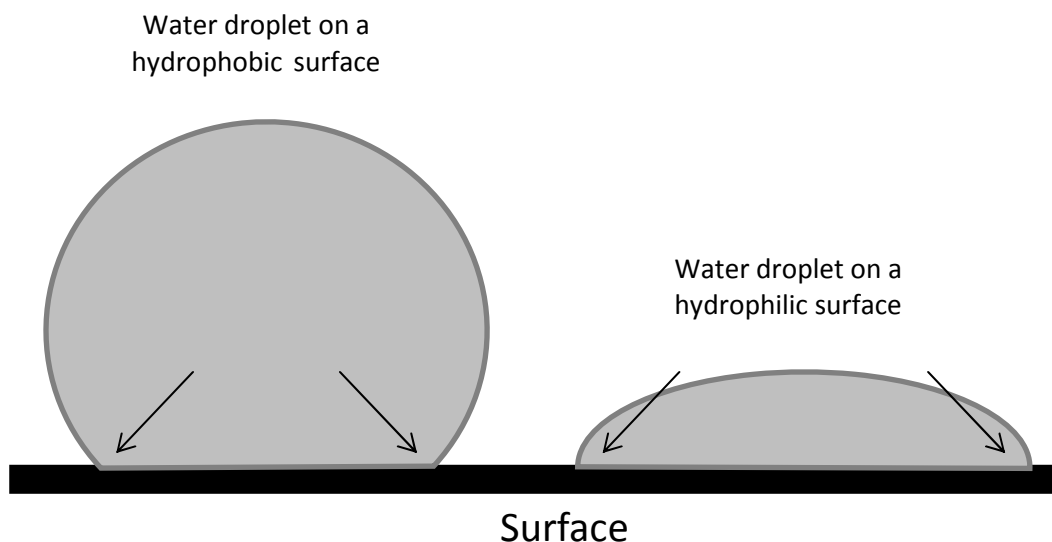


Figure 3: Shapes of water droplets placed onto non-absorbent surfaces. Herein represented are the general shapes of water droplets placed onto a non-absorbent hydrophobic and hydrophilic surfaces, respectively. They exhibit the shape of a truncated sphere. The arrows indicate the liquid phase of the triple contact point (air/water/surface) where the contact angle is measured.

Contact angles greater than 90° indicate that the surface is very hydrophobic and that the aqueous solution interacts very poorly with molecules on the surface, while contact angles less than 60° indicates that the surface is hydrophilic and the aqueous solution interacts well with the surface. Surfaces with contact angles between 60° and 90° can be considered as intermediately wetting surfaces; these surfaces are somewhat hydrophobic but are definitely not hydrophilic. The most direct method to obtain the contact angle of a droplet on a surface is to make use of a magnifying optic with crosshairs attached to a goniometer (36). With the advancement of technology, however, this process is now digitized and automated with computer algorithms that calculated contact angles by analyzing droplet shapes in real-time. This, however, is typically useful for angles greater than 30° as angles smaller than this can be difficult to measure. For

superhydrophilic, non-absorbent surfaces, where the contact angles are between less than 30° , an alternative method based on the diameter of the droplet on the surface can be used to calculate the contact angles (36,37).

1.6. Hardness of Polymers

The hardness of polymer can be quantified using a Shore hardness scale. There are many different Shore scales, of which the most commonly used are: OO, A, and D. The Shore OO scale can be used to measure soft polymers (e.g., gummy bear candies), Shore A for medium hard polymers (e.g., automobile tires), and Shore D for very hard polymers (e.g., polymer shell of hard hats). Shore readings are taken using a durometer and it has an indenter which is pressed into the polymer body. The reading taken is essentially the resistance of the polymer body to the indenter: a gauge displays the hardness reading.

The harder the polymer, the more resistance the indenter experiences, and the greater the Shore reading on the gauge. A reading of 0 indicates there is no resistance to the indenter and the polymer is softer than that particular Shore instrument's working range. Conversely, a reading of 100 indicates there is no penetration into the polymer by the indenter. A Shore OO reading of 10 is approximately the hardness of a gummy bear candy while a reading of 75 is approximately the hardness of a pencil eraser.

The hardness of acrylic polymers is readily controlled by the character of the ester alkyl group. Typically, as the size of the alkyl group increases, the hardness of the resulting acrylic polymer decreases. For example, PMMA is the hydrophobic homopolymer of methyl methacrylate that is very hard and rigid. By contrast, poly(butyl methacrylate) PBMA, the homopolymer of butyl methacrylate, is soft and pliable. Other

acrylic esters, with even larger groups such as 2-ethylhexyl are also widely used in commerce.

The hardness of polymers originates from the packing of the polymer chains, and this is affected by the side groups associated with the monomers. With aliphatic side groups, longer and larger groups prevent the uniform packing of the polymer yielding lower densities and softer polymers, while shorter chains can allow for closer packing will yield higher densities and harder polymers.

2. Proposal

The target of this project is to develop methacrylate polymers that possess tuneable properties. By being able to vary the properties with a high degree of control, it should be possible to screen the polymers against various biological agents (e.g., bacteria, cells, and proteins) to gain an insight into the properties of the polymer for the specific application. The polymers will ideally be targeted as biomaterials. Of the numerous properties available for investigation, the two properties to be particularly explored are surface wettability and hardness.

The key monomer that we chose to examine is the polymerizable trisiloxane surfactant, ACR A008-UP (ACR) (Figure 4). This monomer possesses both a long ester chain, and a chain that is highly hydrophilic. Our hypothesis was that its incorporation into a methacrylic polymer chain would affect both wettability and hardness. It was further hypothesized that the degree of hydrophilicity and softness would track with the mole fraction of the ACR monomer in the synthesized polymers.

PMMA is an exceptionally hard polymer. To provide an independent way to manipulate the hardness of the polymeric system, it was decided that butyl acrylate (BMA) could be incorporated in the polymer in (partial) place of MMA. By increasing the amounts of the hydrophilic surfactant monomer into a hydrophobic system, the resulting polymers should exhibit increasing surface wettability. By varying the amounts of MMA, BMA, and surfactant monomers in the formulation, both the wettability and hardness properties of the resulting polymer can be tuned and explored.

Therefore, the following thesis describes the systematic study of these variables and the way they impact on the properties of the resulting polymers, in particular, the degree to which the surfaces support cell growth.

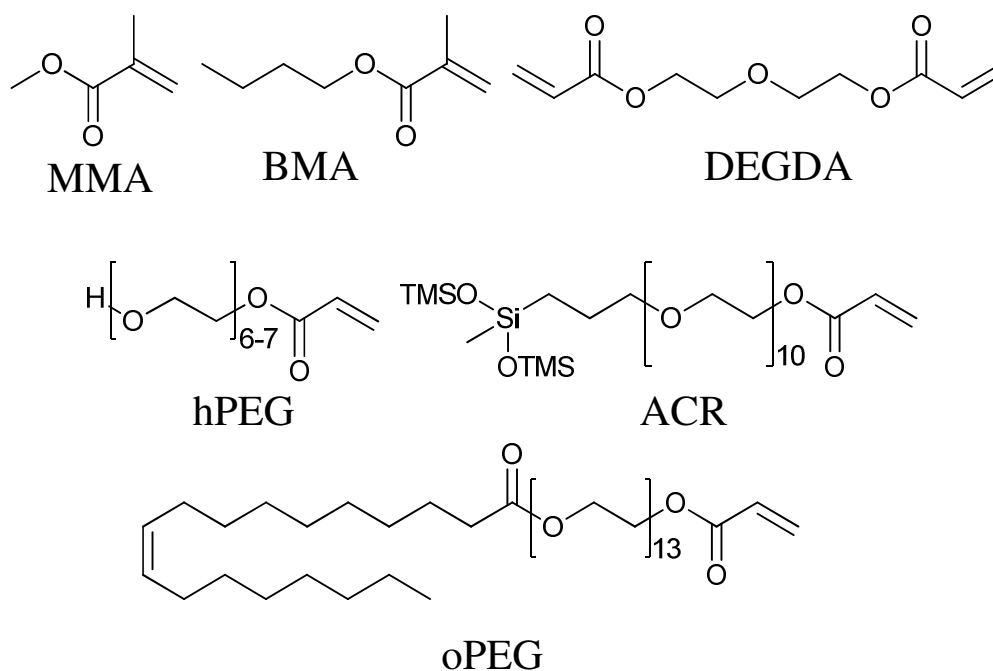


Figure 4: The chemical structures of all the acrylic and methacrylic monomers, and crosslinker. Methyl methacrylate (MMA) and butyl methacrylate (BMA) are methacrylic monomers while PEG-acrylate (hPEG), ACR A008-UP surfactant (ACR), and oleate-PEG-acrylate (oPEG) are the acrylic monomers. Diethylene glycol diacrylate (DEGDA) is the crosslinker.

3. Results and Discussion

3.1. Synthesis of Polymers

The general syntheses of the polymers involved the dissolution of the photoinitiator camphorquinone (CQ, 1 wt%) and the co-initiator that generates the radical ethyl 4-(dimethylamino)benzoate (EDB, 1 wt%) into the chosen quantities of monomers and crosslinker diethylene glycol diacrylate (DEGDA, 1 wt%). The reaction mixture was deoxygenated by bubbling nitrogen through it for 30 s, and then poured into a small Teflon-lined Petri dish before being placed under a blue light source to initiate polymerization, which was allowed to take place for 1 h.

Following the curing process, the polymers were removed from the Teflon-lined Petri dish (peeled away) and submersed into 2-propanol overnight to extract any unreacted materials and low molecular weight oligomers. Following the soaking process, the polymers were removed from the 2-propanol and placed into a vacuum over overnight to dry at 50 °C and 500 mm Hg. After the extraction, a yellow polymer resulted that was submitted to a variety of analysis techniques.

3.2. Polymer Characterization

The polymers were mainly characterized by contact angle measurements as an indication of surface wettability, and Shore OO measurements to probe the polymers overall hardness. Proton nuclear magnetic resonance spectroscopy was used to analyse the extracted material, and scanning electron microscopy was used to observe the surface patterns.

3.3. Spontaneous Surface Structures

After the synthesis, extraction, and the overnight drying of the polymers in the vacuum oven, the majority of the samples revealed an unexpected, ordered pattern at the air interface (Figure 5): the polymer body remained optically transparent. This pattern was visible by the naked eye and has a regular periodicity of approximately 500 μm . The samples uniformly exhibited a kind of crosshatched pattern, or herringbone ‘woven’ pattern, with a bidirectional orientation.

The phenomenon of surface structuring has been reported in a variety of materials ranging from metals to polymers. For example, Chua et al. reported spontaneous formation of ordered structures on poly(dimethylsiloxane) (PDMS) polymer surfaces after it was subjected to oxygen plasma treatment (38). During treatment process, the temperatures were elevated and the silicone expanded in volume and, while in this expanded state, the oxidized surface crosslinked to form a thin layer of silica. As the silicone cooled after the treatment and the expanded silicone body shrinks to its equilibrium volume, the rigid silica layer on the surface buckles into highly ordered structures due to the compressive stress (38).

Similarly, very thin metallic films (< 50nm, in some cases only 5 nm) can exhibit similar phenomena. After coating onto a silicone elastomer and, in some cases, heating of the silicone, coating with the metal film, and recooling, the formation of wave patterns was observed (39,40). However, even when the silicone was not expanded thermally the same type of effect is observed if the metal is sufficiently hot when sputtered: the

metalized surface does not yield, and buckles at stress points resulting and regular patterns (*41*).

Such structuring at the air interface of a polymer is not expected in an isotropically cured polymer. We hypothesize the spontaneous formation of a cross-hatched pattern is due to a preferential curing of the polymer surface. The curing should proceed preferentially in a top-down fashion, as the intensity of the light attenuates as it passes through the polymer body (Figure 6). This results in a gradient of light intensities generating a more crosslinked upper layer relative to the middle and lower strata of the polymer body. Accompanying the higher crosslink density is a more rigid layer. As the reaction mixture shrinks during polymerization the top layer should preferentially buckle under compressive stress while the materials below, with lower degrees of polymerization and lower rigidity, should yield under the compressive stress. This hypothesis is consistent with the theories proposed by Chua et al. and Bowden et al. even though the method of forming the rigid surface varies (*38-40*).

The surface structures present interesting phenomenology. In addition, it is known that surface roughness, although typically at much small length scales, can affect the ability of cells to adhere and proliferate. We have not specifically examined the surface structuring properties on cellular behaviour.

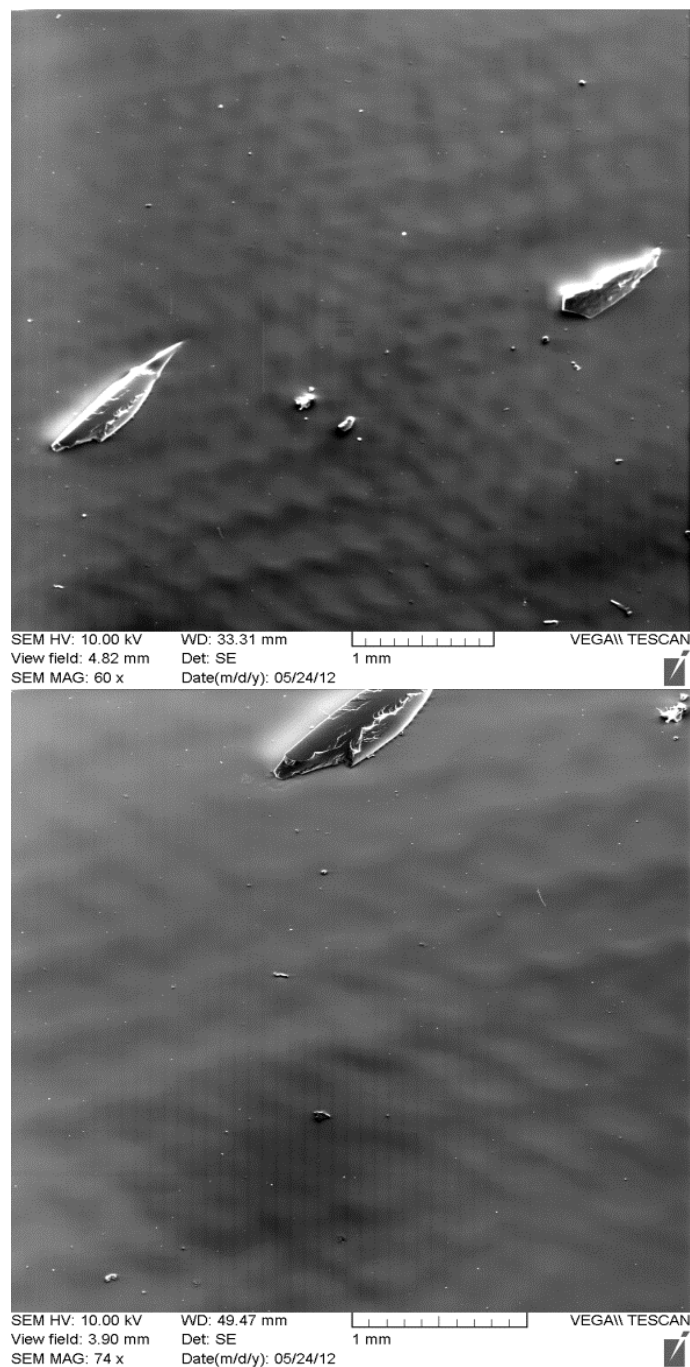


Figure 5: SEM images of the spontaneous surface structures. These spontaneous structures formed due to the preferential curing of the polymer surface followed by a buckling event due to compressive stresses caused by a shrinking middle and lower polymer body. The periodicity of is approximately 500 μm .

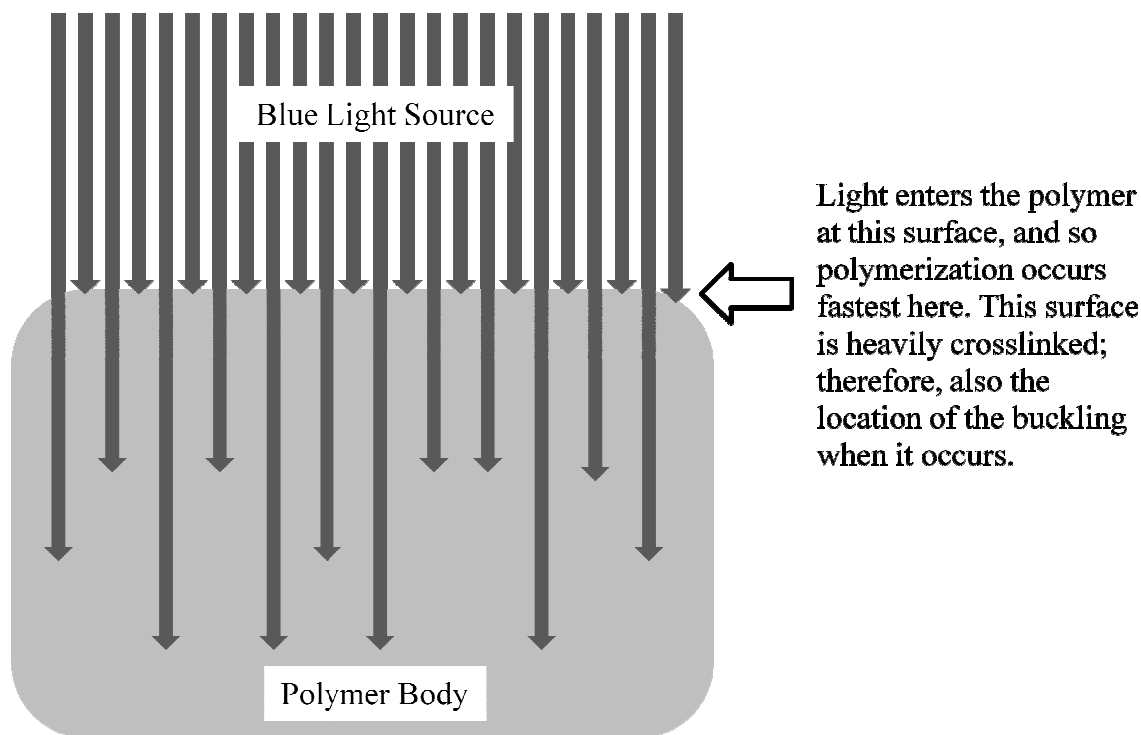


Figure 6: Differences in light penetration of the polymer body. More light penetrates the upper layer of the polymer than compared to the middle and lower strata. This results in a more crosslinked surface than the rest of the polymer body.

3.4. Hardness of ACR-MMA-BMA Polymers

The hardnesses of the polymers produced by photopolymerization are related to their molecular structure, which influences the physical and intra/intermolecular interactions between polymer chains. Polymers with low molecular masses are generally softer and not brittle: high molecular masses will generally yield polymers that are tougher (42). The interactions between polymer chains can sometimes lead to crystalline regions in the polymer as a result of neat and ordered packing of the chains due to intramolecular and/or intermolecular interactions. For example, Gracias et al. reported the hardness of polyethylene and polypropylene polymers is proportional to crystallinity of the polymer; the more crystalline the polymer, the harder it becomes (43).

In poly(methacrylic) homopolymers, the R-group (Figure 7) affects the overall hardness of the resulting polymer. Generally, the smaller the R group, the harder the polymer. This can be observed indirectly through the glass transition temperature (T_g) of the polymers. In Table 1, the T_g of selected poly(methacrylic) homopolymers shows that as the R-group increases in size, the T_g drops.

Polymer reinforcement can arise from other types of interactions. Park et al. synthesized a hard-soft block copolymer using poly(urethane) (PU) and PDMS (44). As PDMS is a highly mobile chain with limited interactions with other chains, it forms the soft segment of the block copolymer, while PU is a rigid and linear polymer that is capable of hydrogen bonding with other PU blocks resulting in hard segments. The affiliation of the hard blocks leads to a physical crosslinking that rigidifies the polymer

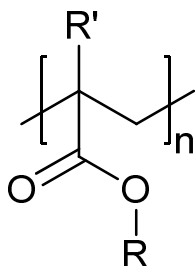


Figure 7: The general chemical structure of a poly(acrylic) ($\text{R}' = \text{H}$) and poly(methacrylic) homopolymer ($\text{R}' = \text{CH}_3$).

Table 1: Glass Transition Temperatures for Selected Poly(methacrylic) Homopolymers (R = Me, Figure 7)^a

R-group	T_g (K)	T_g (°C)
Methyl	378	103.85
Ethyl	338	63.85
<i>i</i> -Propyl	354	79.85
<i>n</i> -Butyl	293	18.85
<i>n</i> -Hexyl	268	-6.15

^a T_g values are adapted from (45).

As polymers become softer, they often gain some degree of adhesiveness. For example, PMMA, which is hard at room temperature, is not adhesive while PBMA, which is soft at room temperature, is tacky. The factors that affect the adhesion to surfaces are widely unknown at this moment and all commercial research into adhesives for applications generally follow an empirical approach (46). Good adhesives must operate above their T_g . Of course it is not necessary to perform adhesive polymers to a substrate: they can also be polymerized directly on the substrate surface (47). The degree of adhesion of polymers can be controlled over wide range. One class of particularly adhesive polymers is known as pressure sensitive adhesive (PSA) materials, which are polymers that are inherently tacky once they are cured. Applications of these pressure sensitive adhesives can be found everywhere around the common household from the backs of sticky notes, bandages, and stationary tapes. Both silicones and acrylics can be formulated into pressure sensitive adhesives.

Modern PSA are soft, viscoelastic materials that adhere to surfaces upon contact, and adhesion is maintained due to the fact that the net energy required to break the adhesion is greater than the forming process (46). When the surfaces are in the process of

being separated, fibrillation of the adhesive occurs—these fibrils are related to the strength of the adhesion. Zosel reported that fibrillation is related to the entanglement network and crosslink densities—the higher the entanglement, the increased number of fibrils and the stronger the adhesion; however, if the crosslink density is higher than the entanglement density, then it suppresses the formation of fibrils (48).

Acrylic PSAs are generally random copolymers of *n*-butyl acrylate or 2-ethylhexyl acrylates, which have long R-groups (Figure 7) leading to low glass transition temperatures. Acrylics with small R-groups like MMA and tackifiers can be added to tune T_g , and methacrylic acid can be added to improve adhesion (46) by changing the nature of chemical interactions at the substrate interface.

Based on the T_g given in Table 1, it is expected that PMMA will be harder than PBMA. For the ACR monomer (Figure 4), its R-group is significantly longer than that of MMA and BMA, it is hypothesized that poly(ACR) (PACR) will exhibit a T_g that is much lower than PMBA, which also suggests derived polymers will be softer at any given temperature. Similarly, as Creton mentioned in reference 46, MMA was used herein to tune the T_g of the resulting polymers which directly affects the hardness of the polymers.

At a given weight percent of ACR to methacrylate monomers, the ACR-MMA polymers were found to be harder than those of ACR-MMA-BMA and ACR-BMA, with the latter being the softest (

Figure 8). PMMA, PBMA, and PACR have Shore OO hardness readings of 97, 81, and 75, respectively. In all three formulations, the hardness of the polymers decreased as the percentage of ACR increased. This expected outcome can be correlated to ACR being

a monomer that leads to low T_g polymers, which contributes relatively small amounts to the overall hardness of the polymer than compared with MMA.

Shore OO Hardness of ACR-Methacrylate Polymers

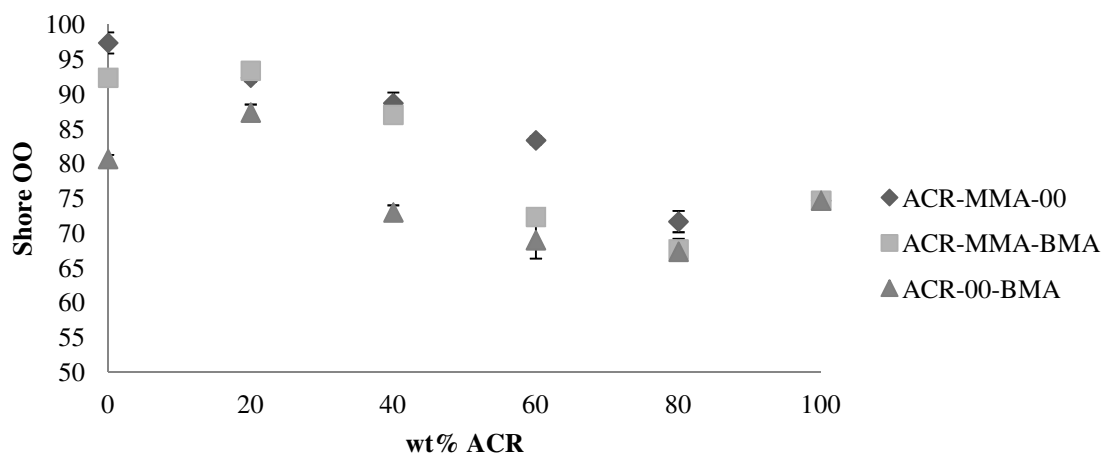


Figure 8: Shore OO hardness of ACR-methacrylate polymers.

As ACR-MMA and ACR-BMA polymers both contain ACR, a monomer that leads to soft polymers, at a given ratio of ACR, the copolymers of ACR-MMA will be harder than those of ACR-BMA, as MMA contributes a greater hardness to the modulus than other monomers. On the other hand, ACR-MMA-BMA terpolymers contain two monomers that lead to softer polymers—ACR and BMA, and one that leads to hard polymer—MMA. Therefore, at a fixed fraction of ACR, the ACR-MMA-BMA polymers will be softer than the ACR-MMA polymers but harder than the ACR-BMA polymers. Depending on application of the final polymer, the hardness of the polymers can be tuned by altering the percent composition of ACR. In conclusion, co- or ter-polymers of different hardness can be produced predictably by judicious modification of the starting

formulation. The impact on polymer hardness was found to occur in the order $ACR < BMA < MMA$.

3.5. Extractions of ACR-MMA-BMA Polymers

As these polymers could be potential biomaterials for implants, it was important to ensure any possible extractable materials were extracted from the matrix of the polymer prior to their conversion into a device. It is also important to note that all analyses of the final polymer products were completed after this extraction process. This is particularly important, as ACR contains a trisiloxane head group and various literature reports suggest there is toxicity associated with free trisiloxane-based superwetters, at least to various insects and mites (49-57). It is expected that any unreacted monomers and low molecular weight oligomers would be removed from the matrix by overnight Soxhlet extractions. However, it was of interest to ensure that the extraction process was complete and to identify the extracted materials.

Various ACR-MMA-BMA polymers were extracted with 2-propanol overnight in a Soxhlet extractor, dried in a vacuum oven: their differences in weight prior to and following the extraction are reported. After the first extraction, 20-30% of the original weight was lost, and this was a significant amount of material. However, it appeared that all extractable material were removed from the polymer matrices during the first overnight Soxhlet extraction cycle, as the subsequent percent weight losses were insignificant (less than 5%) (Figure 9).

According to the NMR of the extracted material (Figure 10), the starting materials were either completely consumed by the reaction, or are present in quantities below the

detection limit of the spectrometer. Figure 10 lacks the signals between $\delta = 5.5\text{-}6.5$ ppm that correspond to the vinyl hydrogens of the surfactant (Figure 11), MMA (Figure 12), or BMA (58). It appeared that the material extracted were merely oligomers of the starting material. Studying the oligomers by NMR, the mole ratios of monomers incorporated were approximately the same mole ratios within experimental error indicating that the polymerization is capturing the available starting material (Table 3).

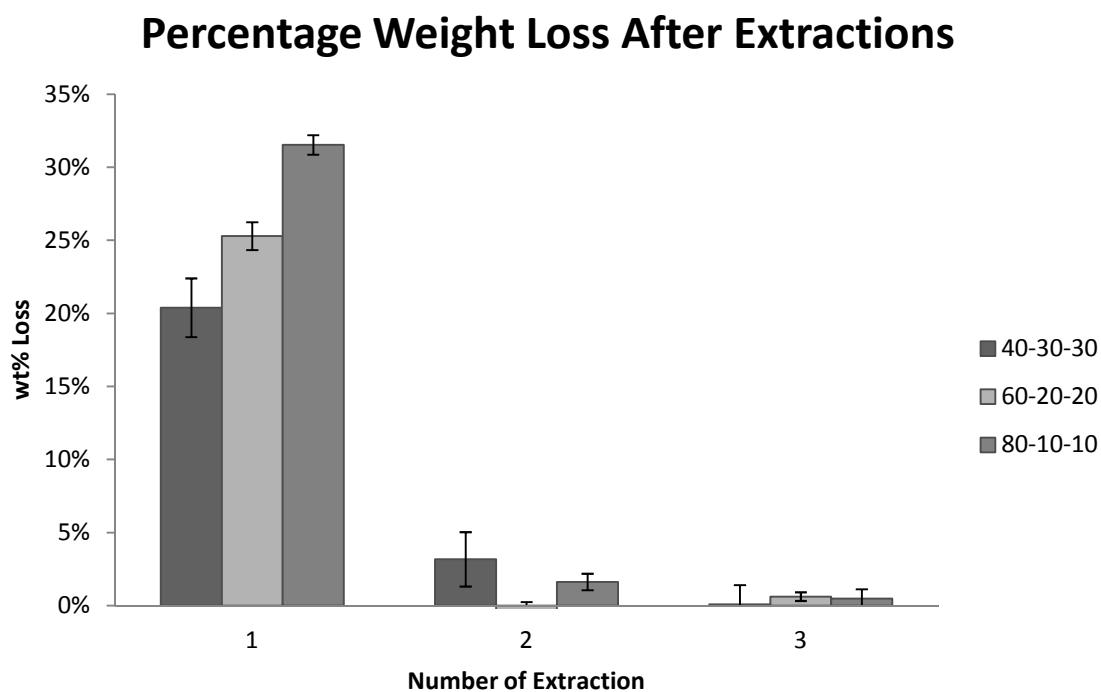


Figure 9: Percent weight loss after subsequent overnight extractions in 2-propanol, and overnight drying in a vacuum oven (50 °C, 20 mm Hg).

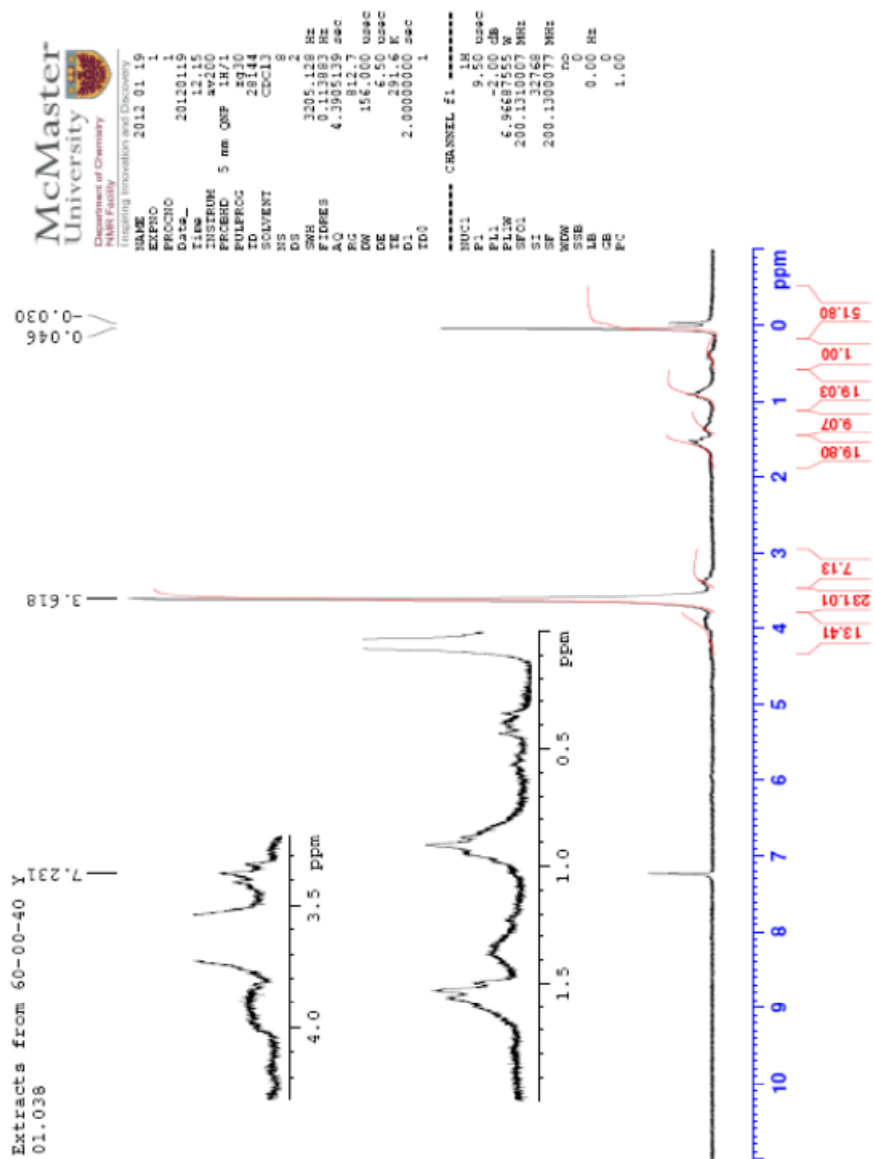


Figure 10: The NMR spectrum of the extracted material.

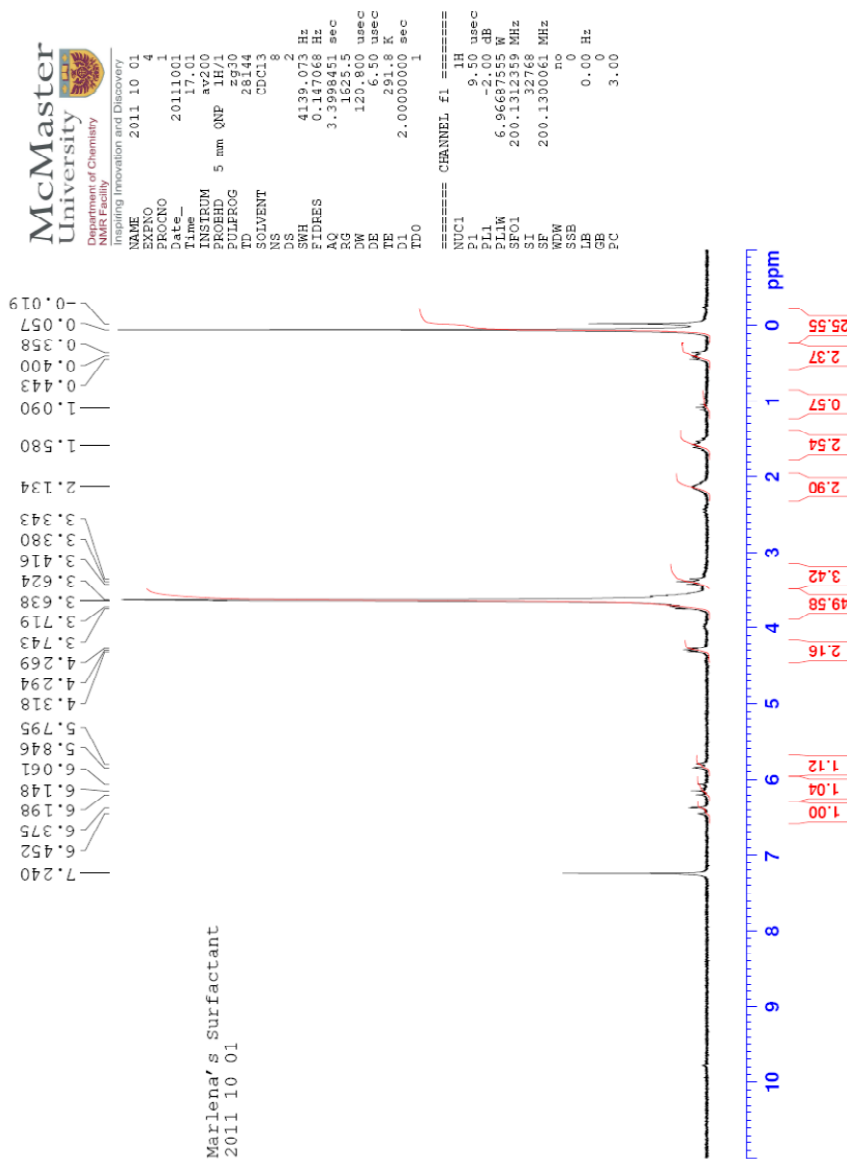


Figure 11: The NMR spectrum of the ACR-A008 UP surfactant monomer. The three vinylic protons located between $\delta = 5.5$ -6.6 ppm.

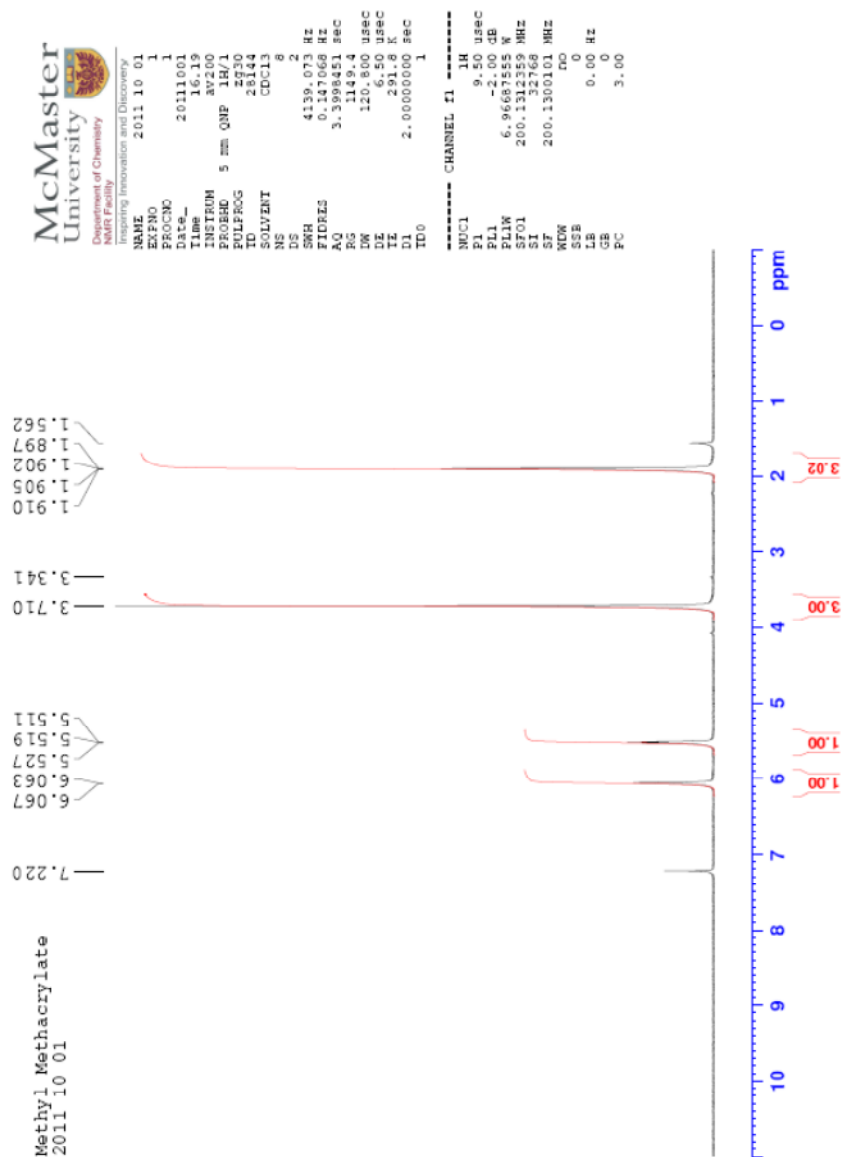


Figure 12: The NMR spectrum of methyl methacrylate. The two vinylic protons located between $\delta = 5.5$ - 6.5 ppm.

3.6. Wettability of ACR-MMA-BMA Polymers

Normally poly(acrylates) and poly(methacrylates) are hydrophobic in nature if the R-group is aliphatic. PMMA and PBMA, whose R-groups are methyl and *n*-butyl respectively, have contact angles between 65° and 75°, respectively, (Figure 13) and are considered relatively hydrophobic by this regard. In order to produce poly(acrylates) and poly(methacrylates) with increased wettability, acrylic and methacrylic monomers bearing hydrophilic R-groups, like PEG, can be incorporated. For example, Chen et al. created wettable poly(acrylates) triblock copolymers with PMMA end blocks sandwiching a random copolymer of PEG-acrylate and poly(acrylic acid) (PAA) (**59,60**). Similarly, PDMS is a silicone elastomer that has many potential applications in the medical field; however, due to their inherent hydrophobicity, proteins have an affinity for its surface, which can be lead to undesired biological effects (**61,62**). Chen et al. also showed by grafting PEG molecules onto the PDMS, the surface will become more wettable (**63,64**).

Ulbricht et al. observed the wettability of PEG-grafted surfaces and reported that the wettability of the surfaces increased as the grafting density of PEG increased (**14**). However, when using a grafting process, there is always a maximum density of PEG that can be grafted on the surface. According to Kingshott et al., grafting of PEG to surfaces using cloud point conditions will maximize the density of the PEG with, of course, other factors such as temperature, salt concentration, PEG chain length, and grafting site density also playing a role (**65**). At higher temperatures and increased salt concentrations, PEG becomes less soluble in solution and therefore reduced interchain repulsion allow

closer packing of the PEG at the substrate interface. Shorter chains also allow for a higher grafting density. Lastly, if assuming every grafting site available can be occupied, the denser the grafting sites, the denser the immobilized PEG brush will be (65).

However, an alternative strategy to create a series of surfaces with different densities exists, the bulk polymerization method that we used to synthesize our polymers. To establish the range of wettabilities available, a series of homopolymers (PACR, PMMA, PBMA, PhPEG, and PoPEG) and a variety of copolymers of ACR, MMA, BMA, hPEG, oPEG were prepared. As expected, in hPEG-methacrylate polymers, as the concentration of hPEG increases in the formulation, the wettability of the surface also increases – essentially linearly – as depicted by the decreasing contact angles in Figure 14. This coincides with the observations of Ulbricht et al. (14). Conversely, when hPEG was substituted by oPEG, which bears a large hydrophobe at the terminus of the PEG chain, the surface wettability of the analogous series of polymers decreased as the concentration of oPEG increases, as seen in the increasing contact angles of Figure 15.

Comparing hPEG to oPEG, hPEG contains a PEG chain terminated by a hydroxyl group which is hydrophilic, conversely, oPEG contains a large and hydrophobic oleate terminating group. Now, it is obvious why increasing the concentration of hPEG will depress the contact angles of the resulting polymers in the series (Figure 14), while increasing the concentration of oPEG will augment them (Figure 15). Largely, the data of both series follow an obvious descending and ascending trend for hPEG and oPEG respectively, but extreme deviations from this trend was observed at the end point, particularly of the oPEG curve. The origin of this deviation from linearity is not clear.

However, we propose that at higher concentrations, there is an association of the highly insoluble oleate groups that precipitate on the polymer substrate surface such that only the PEG portion of the chain protrudes into the air/water interface leading to reduced contact angles (Figure 16). This hypothesis has not yet been challenged. With this data in hand, it was possible to attempt to tune the wettability by creating co- and terpolymers using an intermediate sized hydrophobe, like trisiloxanes, in lieu of the hydrophilic hydroxyl or the largely hydrophobic oleate termini.

In the analogous polymer series, using ACR instead of hPEG and oPEG, the wettability profile was expected to be an intermediate between those of hPEG and oPEG. As predicted, while the percentage ACR monomers increased, the wettability of the surface increased due to the increased presence of PEG on the surface, though only to a threshold concentration of approximately 60 wt% ACR. Curiously, once the threshold concentration was passed, the wettability of the surface decreased once more (Figure 13).

An explanation to the observed phenomenon is proposed in Figure 17. At ACR ratios lower than the threshold concentration, the surfaces become increasingly wettable as more surfactant molecules are presented at the surface for water droplets to interact with. When the surface is dry, the hydrophobic trisiloxane head groups are driven to the air-surface interface as this minimizes energy, similar to Figure 16 (inset). To interact with the water molecules, it is proposed that the surfactant molecules must first reorient themselves so that the PEG chain interacts with the water at the air/water interface while the trisiloxane head group either resides at the water/air/surface interface or – when under water – the siloxane group anchors onto the surface away from water (Figure 17).

Analogous behaviour was not observed from the much larger oleate hydrophobes (Figure 16), which remain adsorbed on the surface. As the density of ACR molecules on the surface increased, more PEG chains were exposed and could interact with the water, which facilitates the spreading of the water across the surface. Once the threshold concentration is passed, however, the ACR molecules become increasingly unable to reorient themselves towards the water, as the ACR density is high. This inability to reorient themselves into a favorable position to expose the PEG chain leaves the hydrophobic trisiloxane head groups exposed to the water, and this leads to the decrease in wettability as the water molecules rather associate with itself. Essentially a hydrophobic brush structure is formed that is highly water repellent.

When polymers are grafted to surfaces at low densities, the polymers are in a random globular form and appear to be adsorbed to the surface from a top-down perspective – this conformation is known as the mushroom regime (Figure 18) (66). The polymers exert minimal repulsive forces on neighbouring polymers because there is enough space between polymers to mediate any such forces. As the density of the graft polymer increases, so do the repulsive forces exerted on the polymer chains as the polymers physically become closer. Eventually, at a particular graft density, the polymers yield to the excessive repulsive forces from each other and straighten out, normal to the surface to which they are anchored, with the unanchored end pointing away from the surface to alleviate the strain. This conformation where the polymers are linear and stretch out away from the surface is known as the brush regime (66). The thickness of the

layer is affected by the molecular weight of the polymer anchored to the surface and the grafting density (67).

In our case, the ACR molecules were increasingly packed together as their surface concentration increased, causing a shift from the mushroom to brush regime. At low ACR concentrations, ACR on the surface exhibits a mushroom regime allowing for easy reorientation when necessary. However, as the concentration continues to increase, ACR molecules become more brush-like, and this hinders the ability of the molecule to reorient itself when exposed to water. This coincides with the observed wettability profile of the ACR-methacrylate based polymers Figure 13.

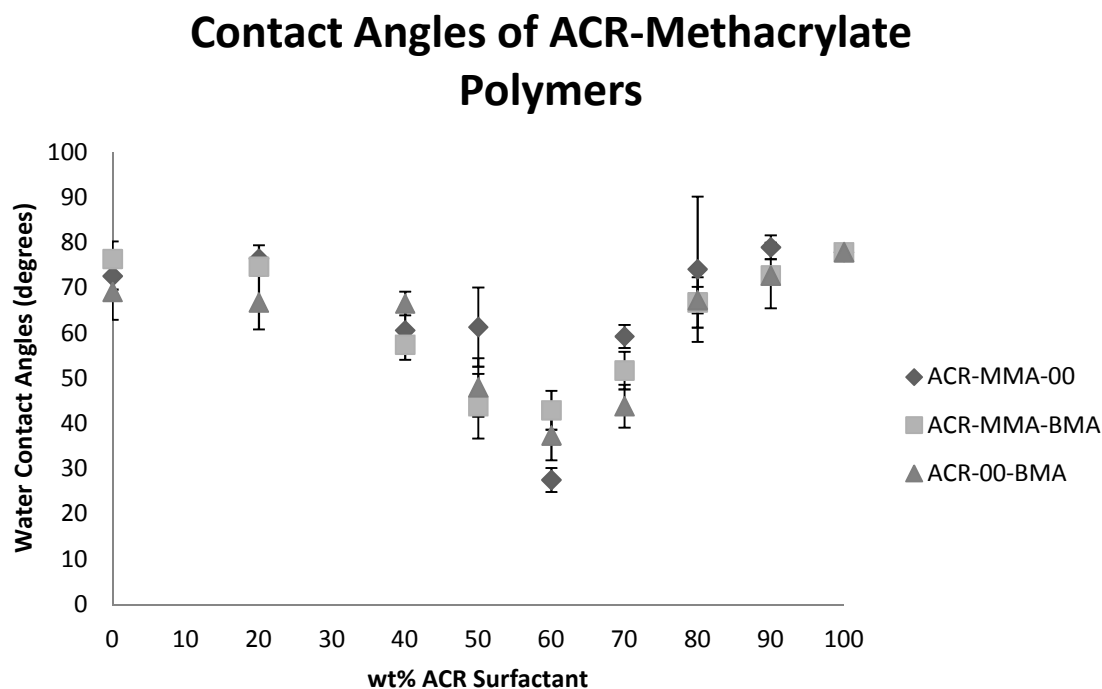


Figure 13: The wettability of ACR-methacrylate polymers.

Contact Angles of hPEG-Methacrylate Polymers

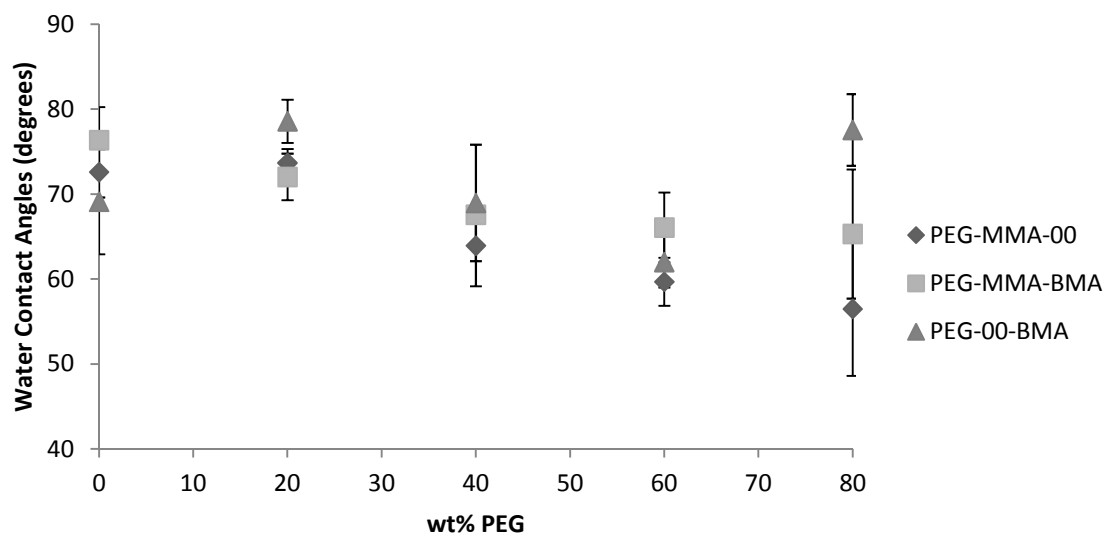


Figure 14: The wettability of hPEG-methacrylate copolymers.

Contact Angles of oPEG-Methacrylate Polymers

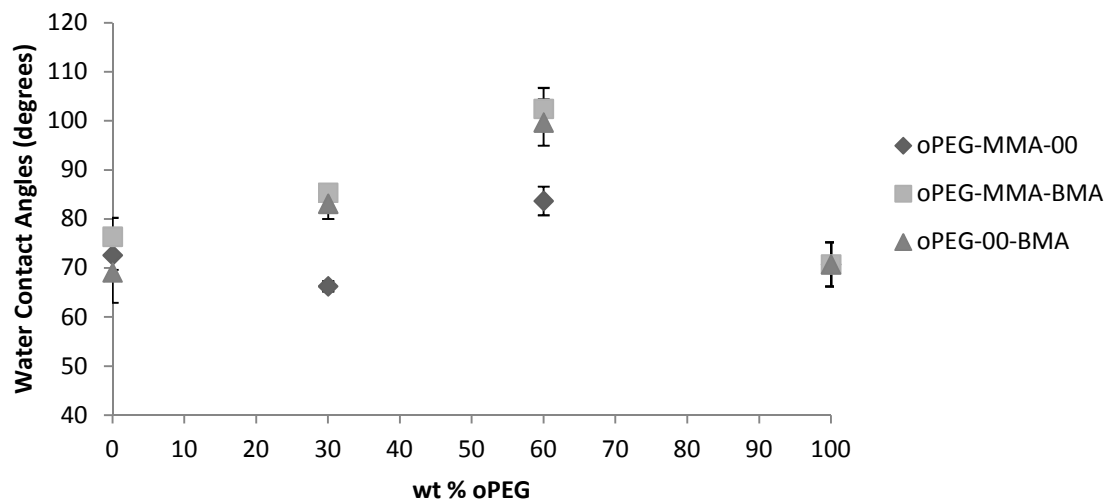


Figure 15: The wettability of oPEG-methacrylate polymers.

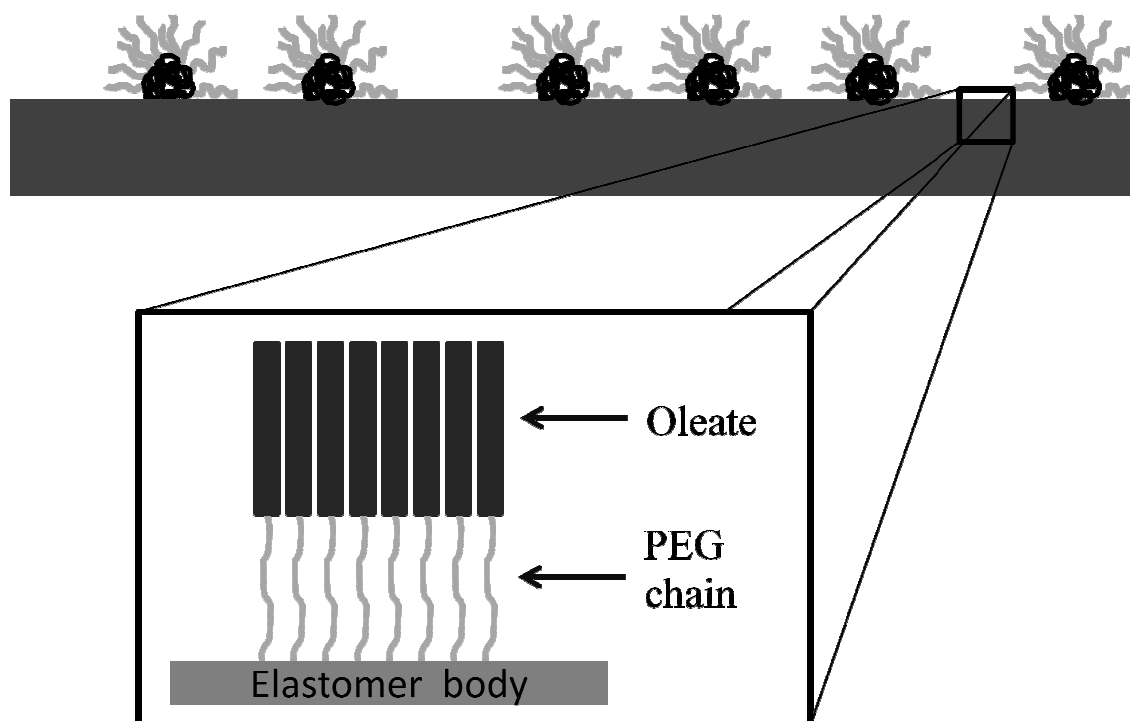


Figure 16: Oleate clusters (black = oleate chain; gray = PEG chain) adsorbed onto the oPEG-methacrylate elastomer surface. The orientation of the oleate and the PEG chains of the elastomer body (inset).

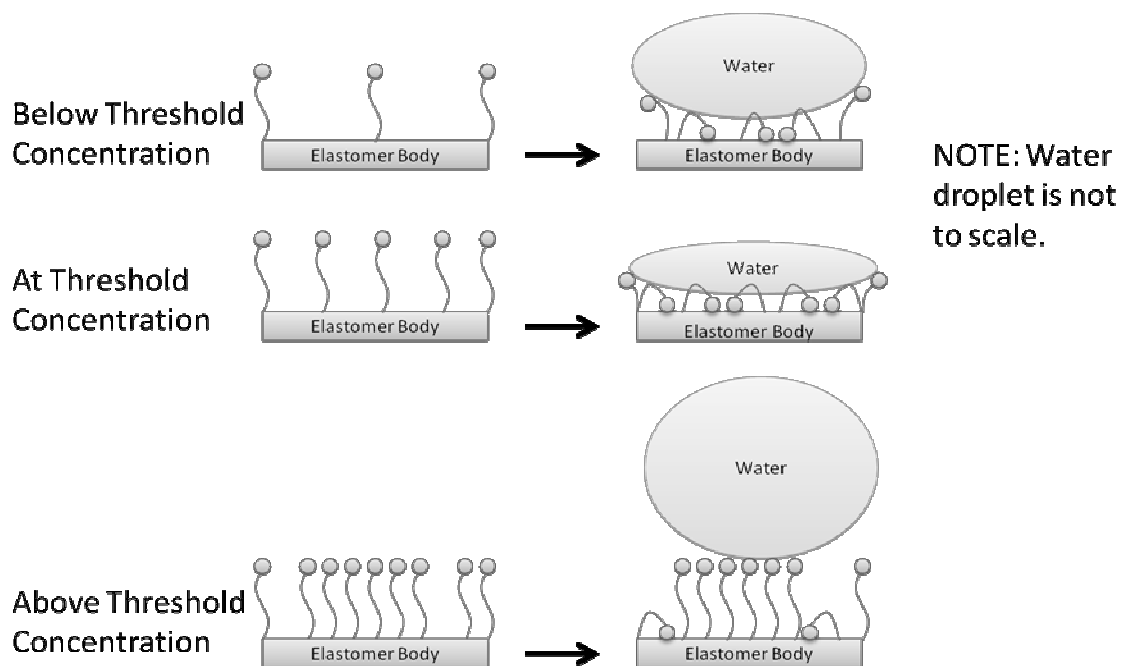


Figure 17: A proposal for the unusual wettability of ACR-methacrylate polymers.

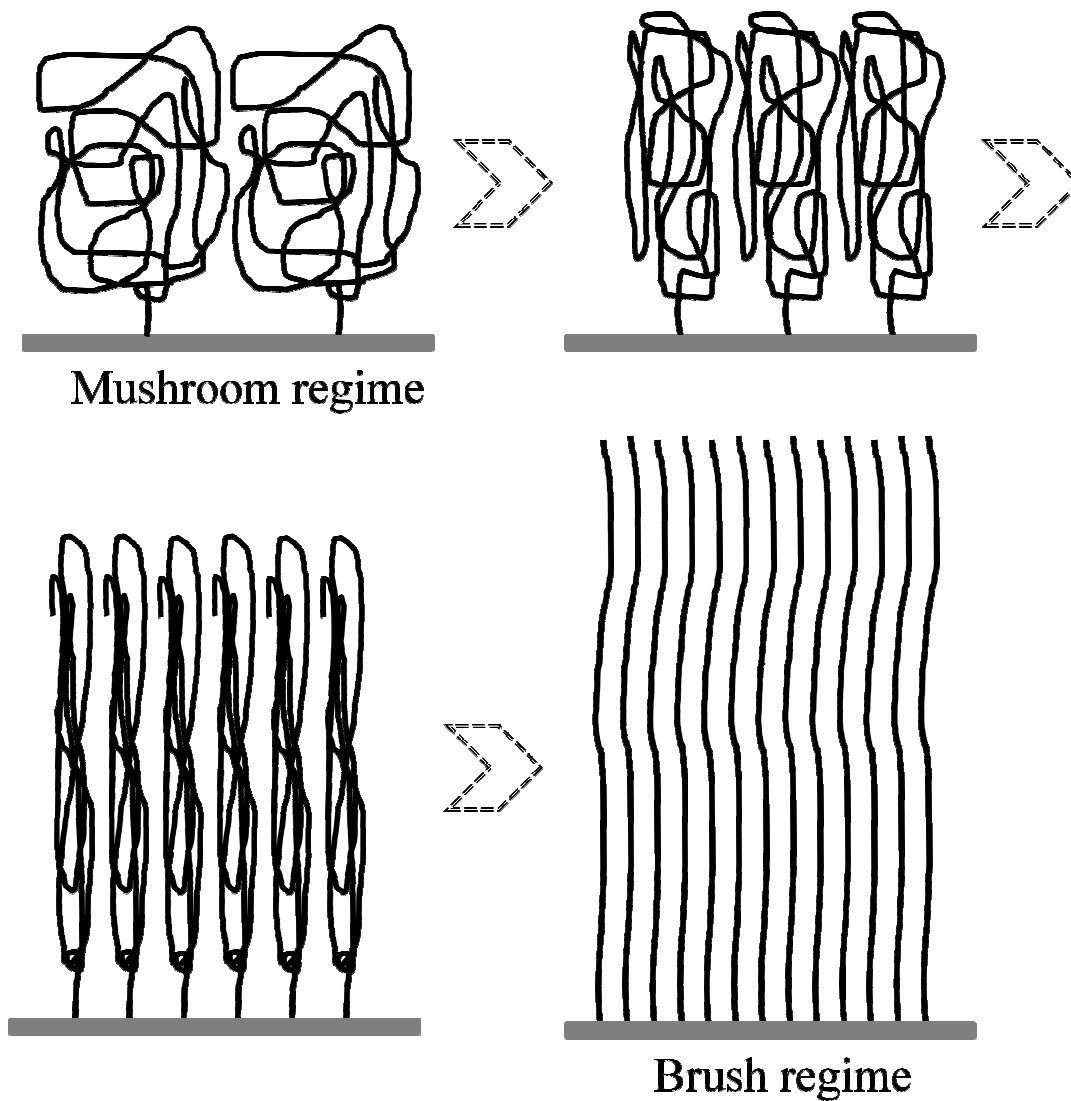


Figure 18: Progression of the mushroom to the brush regime as a function of increasing graft density. Note that the polymer lengths are not to scale and are only for illustrative purposes.

3.7. Stability of the ACR-MMA-BMA Polymer Surface

In aqueous solutions, the siloxane head-groups of the surfactants are known to slowly hydrolyze at neutral pH, but will rapidly degrade under acidic and basic conditions (68,69). Silicones, including the trisiloxanes found at the terminus of the PEG chains in the ACR, are normally hydrolytically stable to water in the atmosphere: as a general rule, bulk water is required for their degradation. The stability of the trisiloxanes is directly related to the wettability of the surfaces. Should hydrolysis occur under normal atmospheric conditions, the trisiloxanes would be converted into silanols, which are more hydrophilic, and the surface wettability should increase. Over a period of three weeks, the wettability of selected surfaces were monitored (Figure 19). The surface wettability appeared to be stable and did not exhibit significant changes suggesting the trisiloxanes head groups are stable under these conditions.

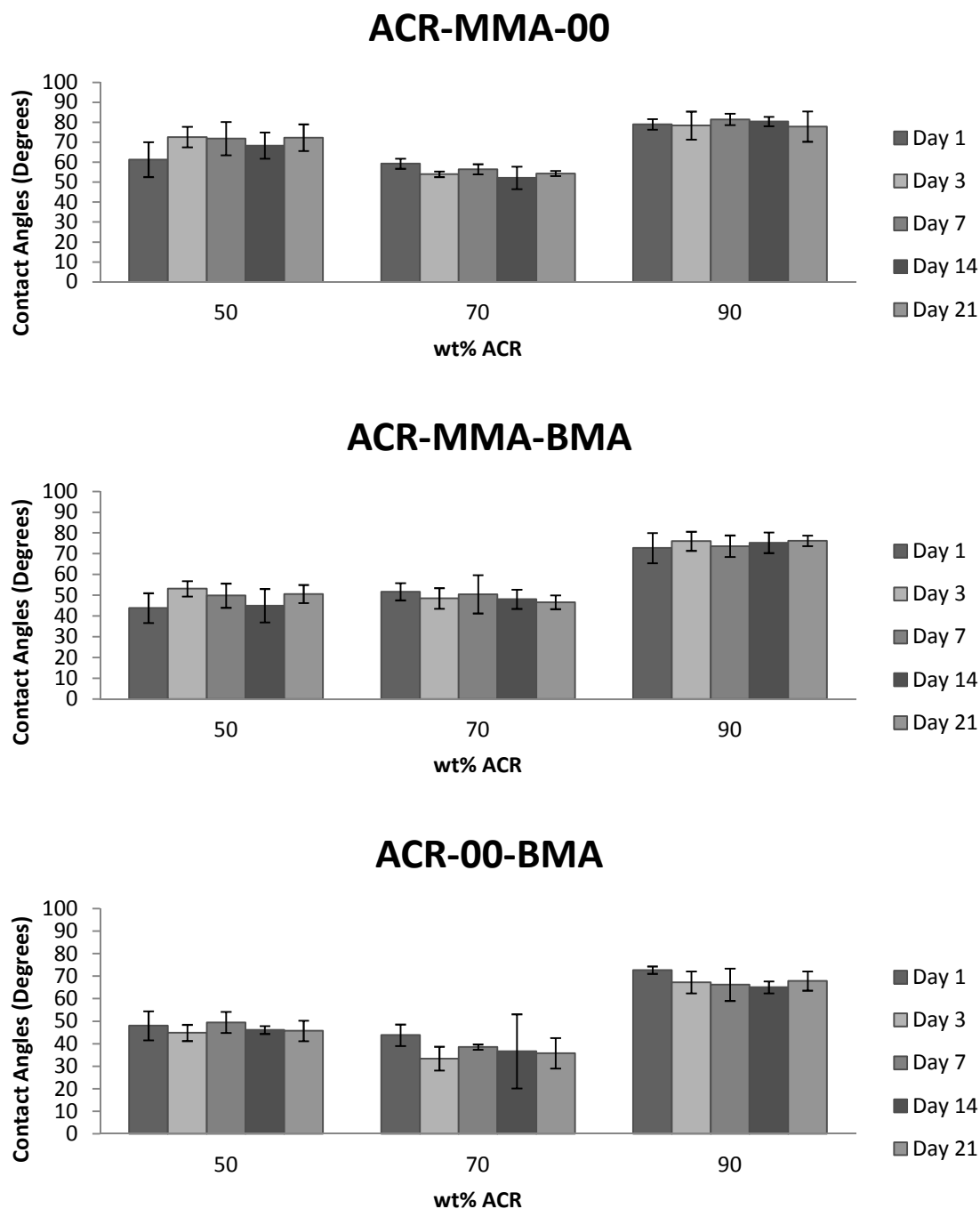


Figure 19: The wettability of selected ACR-methacrylate polymers over a three week period to monitor the stability of the trisiloxane head group. Over this period of time, the wettability of the polymers did not change significantly which implied the stability of the trisiloxane head groups.

3.8. Controlling Surface Properties of Biomaterials

The original objective of this research was to create a suite of materials that systematically varied in their hardness and their wettability by using a polymerization silicone-PEG-acrylate surfactant, ACR A008-UP. We hypothesized that, with the incorporation of MMA and BMA into ACR, we would be able to tune the hardness of the final polymer, and as expected, the hardness can be varied simply by controlling ratio of monomers. As shown in Figure 8, as the concentration of ACR increased, the hardness of the polymers decreased, and likewise, as the concentration of MMA increased, so did the hardness.

The outcome with respect to wettability was unexpected. Initially, a comparison of polymers prepared from MMA, BMA and ACR showed that increased wettability accompanied an increase in ACR concentration. However, this relationship fell down at high ACR concentrations (Figure 13). It was therefore necessary to compare PEG-acrylate polymers that had either no hydrophobe (hPEG), or an organic hydrophobe (oPEG). The hPEG follows an expected pattern: as the hPEG concentration increased, so did wettability. However, the oPEG containing materials also followed an unexpected trend.

At low concentrations, the surface wettability decreased as the concentration of oPEG increased; however, at high concentrations of oPEG, the wettability of the surface increased (Figure 15). It therefore remains to rationalize the differences provided by silicone-PEG and oPEG. We proposed, in the case of ACR, the wettability is related to the ACR molecules ability to reorient to expose the PEG chains in the presence of an

aqueous solution, and its inability to reorient itself at high concentrations of ACR. In the case of oPEG, where the hydrophobe is much larger in size, reorientation was difficult and as the concentration increased, the wettability decreased (Figure 15). We proposed this sudden increase in wettability at high concentrations of oPEG was due to the adsorption of oleate clusters, with the PEG chains on the outside, onto the surface of the elastomer. This leads to an overall increase of PEG chains on the surface and can account for the sudden increase in wettability at high concentrations of oPEG.

This research has shown that the hardness and wettability of these polymers can be readily controlled, and in the scope of contact lens design and fabrication, should provide information that can be used to directly impact the consumers' comfort. Improved comfort is one of the key challenges for contact lenses. We proposed that comfort may be linked to hydrophilicity which, in turn, affects protein deposition and other factors of interaction between the biology of the eye and the surface. Three series of polymers were prepared that exhibit a wide range of hydrophilicities, but also a wide range of surface chemistries that provide a controlled and variable wettability.

With the chemical design aspects of the polymer behind us, it is important to shift the focus of the research to the biological compatibilities of polymers. Cellular, bacterial, and protein biocompatibility to contact lenses should be investigated as adhesion and adsorption of these agents could compromise the comfort, integrity, and safety of the lenses. For example, from the unpublished work of a fellow colleague, ACR appeared to influence the adhesion of *E. coli* adhesion to the polymer surfaces (Appendix). Furthermore, the ideal contact lenses should not allow for the adsorption of tear proteins

to its surfaces, as any build up could lead to discomfort to the consumer. This is a great challenge due to the number of various proteins present in tears which wet and lubricate the eye (70). There is much to be learned about the biocompatibility of these polymer surfaces, but they are beyond the scope of this research thesis. Nevertheless, the biological component of the research can be continued in the future by the successors of the project.

4. Conclusion

By copolymerizing under radical conditions various amounts of surfactants, different wetting profiles of the resulting products were obtained. In hPEG formulations, the contact angles of the surfaces decreased from approximately 70° as the concentration of hPEG increased. Conversely, in the oPEG formulations, the contact angles of the surface increased from approximately 70° as the concentration of oPEG increased. When polymerizing ACR A008-UP (ACR) with methyl methacrylate (MMA) and butyl methacrylate (BMA), we have shown that surfaces with contact angles between 40° and 80° can be synthesized. In the three different ACR formulations explored, the most wettable surface was produced when ACR constituted approximately 60 wt% of the polymer. When the ACR content was below or above 60 wt%, the wettability of the polymer decreased. In addition, by manipulating the relative ratios of ACR, MMA, and BMA, we have shown that the hardness of the polymers can be controlled. In general, the hardness of the polymers increases as the percentage of MMA increases.

We have also monitored the stability of the trisiloxane head groups as they are liable to hydrolysis. By correlating the stability of the head groups to the surface wettability, the head group appeared to be stable over a three week period as the water contact angles did not change significantly. Lastly, we determined that one overnight extraction in 2-propanol was enough to remove majority of the extractable material. NMR analyses of the extracted material reveal they are low molecular weight oligomers.

5. Materials and Methods

5.1. Chemicals

Ethyl 4-(dimethylamino)benzoate (EDB), acryloyl chloride, butyl methacrylate (BMA), camphorquinone (CQ), diethyl ether, diethylene glycol diacrylate (DEGDA), hydroquinone monomethyl ether (MEHQ) inhibitor remover, methyl methacrylate (MMA), poly(ethylene glycol) acrylate ($M_n \approx 375$) (hPEG), poly(ethylene glycol) monooleate ($M_n \approx 860$), and triethylamine were purchased from Sigma Aldrich. EDB, acryloyl chloride, CQ, diethyl ether, DEGDA, MEHQ inhibitor remover, and triethylamine were used as received. MMA, BMA, PEG, poly(ethylene glycol) monooleate had their radical inhibitors removed by passage through a column packed with MEHQ inhibitor remover and stored at 2 °C until used. Silmer ACR A008-UP (ACR) was a gift from Siltech Corporation and was used as received. Photopolymerization was initiated by a blue light source, Kerber Applied Research BlueCure 25, which was graciously provided by Kerber Applied Research Inc.

5.2. Polymer Synthesis

As the syntheses of the various polymers are similar, differing only by the natures of the monomers ACR, hPEG, or oPEG, and quantities added, a general procedure will be described. All polymers synthesized were formed from a total of 2 g in weight of monomers, contained 1 wt% CQ and 1 wt% EDB as the photoinitiating system, 1 wt% DEGDA as the crosslinker, and all monomers in their respective weight percent ratios.

5.3. Synthesis of ACR-MMA-BMA Polymers

CQ (0.02 g, 1 wt%) and EDB (0.02 g, 1 wt%) were weighed into a 10 mL glass test tube. Uninhibited MMA and BMA were added to the test tube followed by the addition of DEGDA (0.02 g, 1 wt%). The reaction mixture was stirred gently to facilitate the dissolution of the solid reagents to give a homogeneous solution. ACR was then added. After the mixture was thoroughly mixed, it was golden yellow in colour. The reaction mixture was deoxygenated by bubbling nitrogen gas, through a glass pipette into the solution for 30 s, and then poured into a small Teflon-lined plastic Petri dish and irradiated for 1 h. Solutions with greater percentages of ACR were found to cure slower than solutions with less ACR. The solid elastomer was then removed from the Teflon-lined Petri dish and soaked in 2-propanol (40 mL) overnight. The elastomer was then removed and dried in a vacuum oven (50 °C, 500 mm Hg) overnight to afford the final product.

Through NMR studies, both the oligomers (from the extracted material) and the polymers contained monomers whose molar ratios reflected the molar ratios of the monomers in the starting material (Table 3Table 4).

Table 2: Formulation for ACR-MMA-BMA Polymers

CQ (g)	EDB (g)	ACR (g)	MMA (g)	MMA (uL)	BMA (g)	BMA (uL)	DEGDA (g)	DEGDA (uL)
0.02	0.02	0.8	1.2	1282.1	0	0.0	0.02	13.7
0.02	0.02	0.9	1.1	1175.2	0	0.0	0.02	13.7
0.02	0.02	1	1	1068.4	0	0.0	0.02	13.7
0.02	0.02	1.1	0.9	961.5	0	0.0	0.02	13.7
0.02	0.02	1.2	0.8	854.7	0	0.0	0.02	13.7
0.02	0.02	1.3	0.7	747.9	0	0.0	0.02	13.7
0.02	0.02	1.4	0.6	641.0	0	0.0	0.02	13.7
0.02	0.02	1.5	0.5	534.2	0	0.0	0.02	13.7
0.02	0.02	1.6	0.4	427.4	0	0.0	0.02	13.7
0.02	0.02	1.7	0.3	320.5	0	0.0	0.02	13.7
0.02	0.02	1.8	0.2	213.7	0	0.0	0.02	13.7
0.02	0.02	1.9	0.1	106.8	0	0.0	0.02	13.7
0.02	0.02	0.8	0	0.0	1.2	1345.3	0.02	13.7
0.02	0.02	0.9	0	0.0	1.1	1233.2	0.02	13.7
0.02	0.02	1	0	0.0	1	1121.1	0.02	13.7
0.02	0.02	1.1	0	0.0	0.9	1009.0	0.02	13.7
0.02	0.02	1.2	0	0.0	0.8	896.9	0.02	13.7
0.02	0.02	1.3	0	0.0	0.7	784.8	0.02	13.7
0.02	0.02	1.4	0	0.0	0.6	672.6	0.02	13.7
0.02	0.02	1.5	0	0.0	0.5	560.5	0.02	13.7
0.02	0.02	1.6	0	0.0	0.4	448.4	0.02	13.7
0.02	0.02	1.7	0	0.0	0.3	336.3	0.02	13.7
0.02	0.02	1.8	0	0.0	0.2	224.2	0.02	13.7
0.02	0.02	1.9	0	0.0	0.1	112.1	0.02	13.7
0.02	0.02	0.8	0.6	641.0	0.6	672.6	0.02	13.7
0.02	0.02	0.9	0.55	587.6	0.55	616.6	0.02	13.7
0.02	0.02	1	0.5	534.2	0.5	560.5	0.02	13.7
0.02	0.02	1.1	0.45	480.8	0.45	504.5	0.02	13.7
0.02	0.02	1.2	0.4	427.4	0.4	448.4	0.02	13.7
0.02	0.02	1.3	0.35	373.9	0.35	392.4	0.02	13.7
0.02	0.02	1.4	0.3	320.5	0.3	336.3	0.02	13.7
0.02	0.02	1.5	0.25	267.1	0.25	280.3	0.02	13.7
0.02	0.02	1.6	0.2	213.7	0.2	224.2	0.02	13.7
0.02	0.02	1.7	0.15	160.3	0.15	168.2	0.02	13.7
0.02	0.02	1.8	0.1	106.8	0.1	112.1	0.02	13.7
0.02	0.02	1.9	0.05	53.4	0.05	56.1	0.02	13.7

Table 3: Ratio of Monomers Incorporated into Oligomers of the Extracted Material¹

Weight Ratio of Monomers		Theoretical Ratio of Monomers Incorporated into Polymer		Measured Ratio of Monomers Incorporated into Oligomer		Relative Integrations	
%wt ACR	%wt BMA	ACR	BMA	ACR	BMA	ACR	BMA
60	40	1.00	3.63	1.00	1.88	51.80	18.87
80	20	1.00	1.36	1.00	2.27	64.67	27.94

¹ To see the constitution of the crosslinked polymer, please see Table 4.

Table 4: Ratio of Monomers Incorporated into Polymers²

Weight Ratio of Monomers			Theoretical Ratio of Monomers Incorporated into Polymer			Measured Ratio of Monomers Incorporated into Polymer		
%wt ACR	%wt MMA	%wt BMA	ACR	MMA	BMA	ACR	MMA	BMA
40	60	0	1.00	11.61	0.00	1.00	13.39	0.00
40	30	30	1.00	5.81	4.09	1.00	7.42	8.09
40	0	60	1.00	0.00	8.18	1.00	0.00	6.84
60	40	0	1.00	5.16	0.00	1.00	4.56	0.00
60	20	20	1.00	2.58	1.82	1.00	4.53	3.02
60	0	40	1.00	0.00	3.63	1.00	0.00	5.64
80	20	0	1.00	1.94	0.00	1.00	3.17	0.00
80	10	10	1.00	0.97	0.68	1.00	2.33	1.00
80	0	20	1.00	0.00	1.36	1.00	0.00	2.29

	Weight Ratio of Monomers			Relative Integrations ³		
	%wt ACR	%wt MMA	%wt BMA	ACR	MMA	BMA
Continued from Above	40	60	0	21.00	40.18	-
	40	30	30	21.00	22.25	32.34
	40	0	60	21.00	-	27.36
	60	40	0	21.00	13.67	-
	60	20	20	21.00	9.05	18.10
	60	0	40	21.00	-	22.54
	80	20	0	21.00	9.52	-
	80	10	10	21.00	7.49	3.83
	80	0	20	21.00	-	9.14

² To see the constitution of the oligomers from which were extracted from select samples, please see Table 3.

³ Please refer to Appendix 7.2 for the NMRs of the select ACR-methacrylate polymers

5.4. Synthesis of hPEG-MMA-BMA Polymers

The synthesis of hPEG-MMA-BMA polymers were essentially identical as described in Section 5.3. The main difference was hPEG was used instead of ACR.

Table 5: Formulation for hPEG-MMA-BMA Polymers

CQ (g)	EDB (g)	hPEG (g)	MMA (g)	MMA (uL)	BMA (g)	BMA (uL)	DEGDA (g)	DEGDA (μ L)
0.02	0.02	1.6	0.4	427.4	0	0.0	0.02	13.7
0.02	0.02	1.2	0.8	854.7	0	0.0	0.02	13.7
0.02	0.02	0.8	1.2	1282.1	0	0.0	0.02	13.7
0.02	0.02	0.4	1.6	1709.4	0	0.0	0.02	13.7
0.02	0.02	0	2	2136.8	0	0.0	0.02	13.7
0.02	0.02	1.6	0	0.0	0.4	448.4	0.02	13.7
0.02	0.02	1.2	0	0.0	0.8	896.9	0.02	13.7
0.02	0.02	0.8	0	0.0	1.2	1345.3	0.02	13.7
0.02	0.02	0.4	0	0.0	1.6	1793.7	0.02	13.7
0.02	0.02	0	0	0.0	4	4484.3	0.02	13.7
0.02	0.02	1.6	0.2	213.7	0.2	224.2	0.02	13.7
0.02	0.02	1.2	0.4	427.4	0.4	448.4	0.02	13.7
0.02	0.02	0.8	0.6	641.0	0.6	672.6	0.02	13.7
0.02	0.02	0.4	0.8	854.7	0.8	896.9	0.02	13.7
0.02	0.02	0	1	1068.4	1	1121.1	0.02	13.7

5.5. Synthesis of oPEG

To a stirring and sealed 500 mL round-bottomed flask, under nitrogen, was added poly(ethylene glycol) monooleate (9.04 g, 0.011 mol, 1.0 eq, $M_n \approx 860$) and dry diethyl ether (250 mL). Once the mixture was homogenized, triethylamine (7.33 mL, 0.053 mol, 5.0 eq) was slowly introduced to the reaction. Then, while stirring vigorously, acryloyl chloride (1.70 mL, 0.021 mol, 2.0 eq) was slowly introduced dropwise to the reaction mixture. A white precipitate formed instantaneously when acryloyl chloride was added to the mixture.

After stirring overnight, rotovap the reaction until a thick, viscous slushy remains. Reconstitute the remains in diethyl ether and filter through a pad of Celite using vacuum filtration to collect the product. Repeat this step two more times. Dry the liquid product using magnesium sulfate and filter out the drying agent using filter paper, rotovap again to obtain the purified product. (9.162 g, 91.62%) of oPEG.

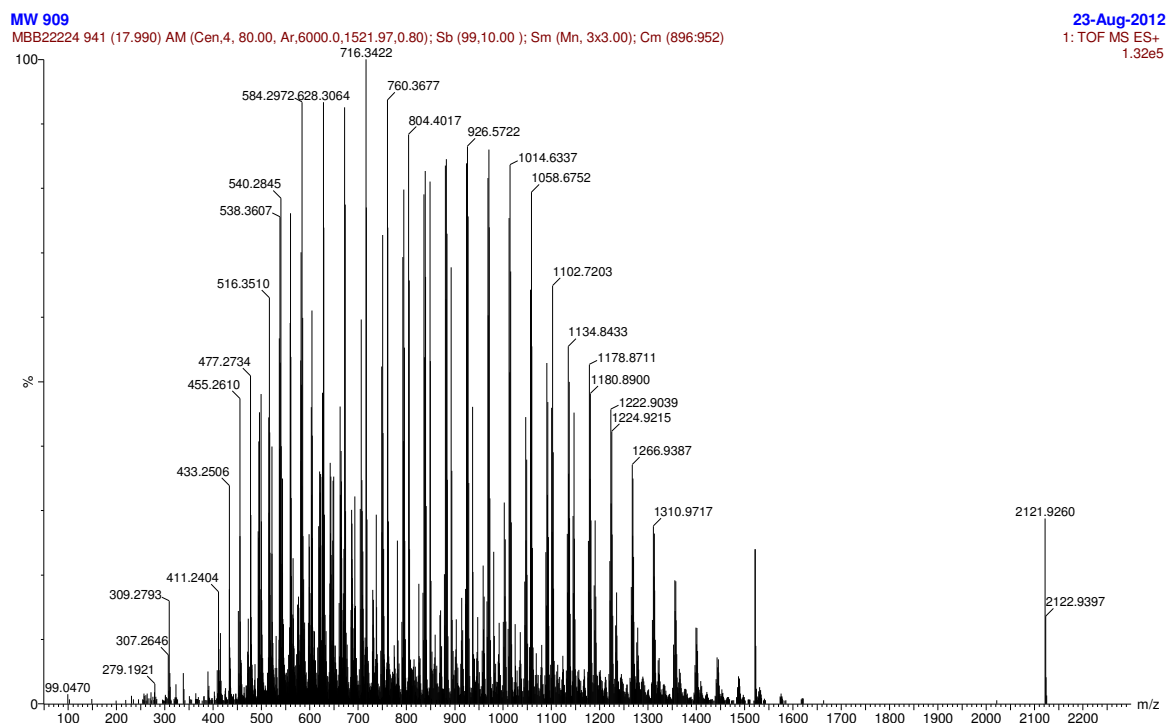


Figure 20: Mass spectrum of oPEG.

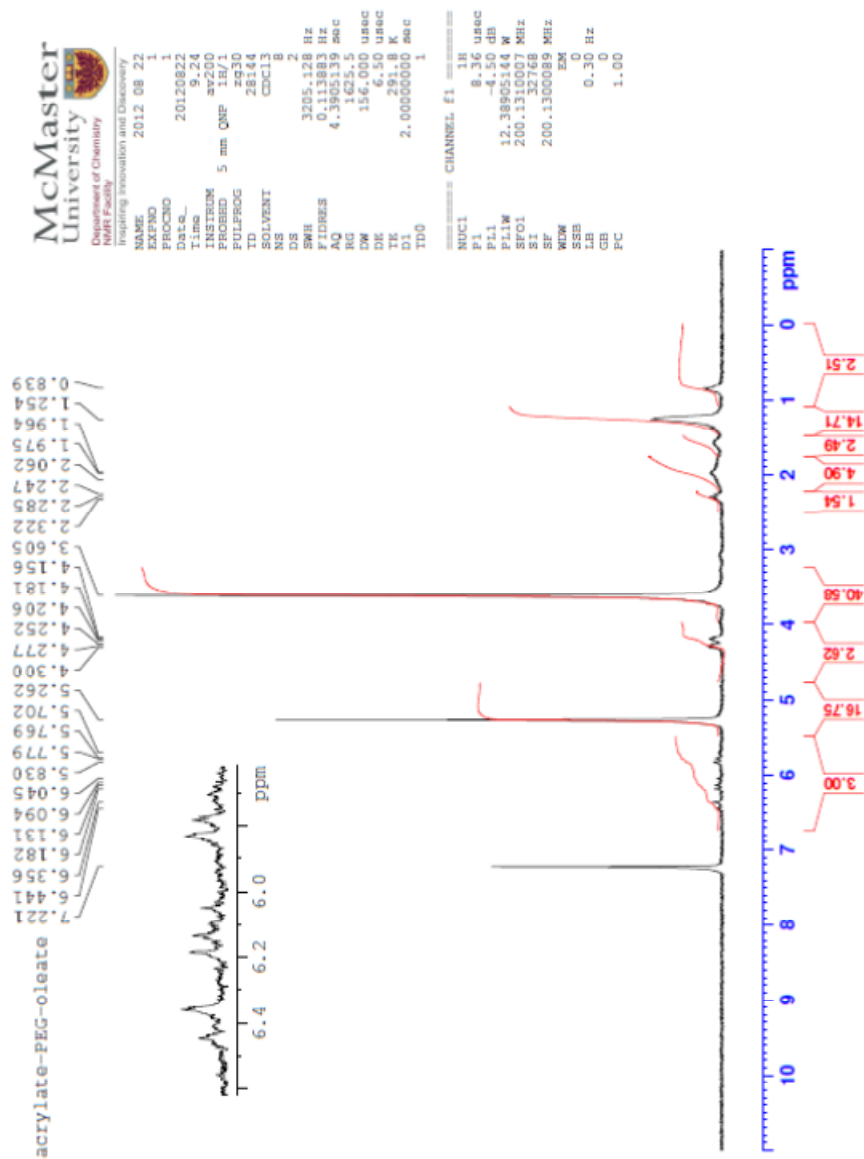


Figure 21: The NMR spectrum of the oPEG monomer.

5.6. Synthesis of oPEG-MMA-BMA Polymers

The synthesis of oPEG-MMA-BMA polymers were essentially identical as described in Section 5.3. The main difference was oPEG was used instead of ACR.

Table 6: Formulation for oPEG-MMA-BMA Polymers

CQ (g)	EDB (g)	oPEG (g)	MMA (g)	MMA (uL)	BMA (g)	BMA (uL)	DEGDA (g)	DEGDA (uL)
0.02	0.02	2	0	0.0	0	0.0	0.02	13.7
0.02	0.02	1.2	0.8	854.7	0	0.0	0.02	13.7
0.02	0.02	0.6	1.4	1495.7	0	0.0	0.02	13.7
0.02	0.02	0	2	2136.8	0	0.0	0.02	13.7
0.02	0.02	2	0	0.0	0	0.0	0.02	13.7
0.02	0.02	1.2	0	0.0	0.8	896.9	0.02	13.7
0.02	0.02	0.6	0	0.0	1.4	1569.5	0.02	13.7
0.02	0.02	0	0	0.0	2	2242.2	0.02	13.7
0.02	0.02	2	0	0.0	0	0.0	0.02	13.7
0.02	0.02	1.2	0.4	427.4	0.4	448.4	0.02	13.7
0.02	0.02	0.6	0.7	747.9	0.7	784.8	0.02	13.7
0.02	0.02	0	1	1068.4	1	1121.1	0.02	13.7

5.7. Shore Hardness Measurements

Shore hardness measurements were taken using a Type OO Model 1600 Rex® Durometer purchased from Rex Gauge Company, Inc. Three small discs were punched out from the main polymer body and stacked, before the hardness reading is obtained. By stacking them, this prevents the durometer from striking the hard surface below and obtaining a false reading.

5.8. Wettability Measurements

Water contact angles measurements were obtained through manual measurements of digital images depicting the water droplets on the surface of the polymers. The images were obtained through the use of a Kruss Contact Angle Measuring Instrument G10 and

the manual measurements were obtained through the use of an angling tool function in GIMP 2.6.8, a GNU image manipulation program. While monitoring the surface using the Kruss instrument, a 3 μL droplet of Milli-Q water was placed onto of the surface of the polymer being examined. A digital image of the water droplet on the surface is captured, and by using the angling tool provided by GIMP, a contact angle was determined by averaging the left and right angles of the droplet.

5.9. Trisiloxane Stability Study

The contact angles of the polymers were measured as outlined in Section 5.8. Following each measurement, the samples were stored in an unregulated paper box in a drawer until they were needed again for the next round of contact angle measurements.

5.10. Soxhlet Extraction

A conventional Soxhlet extractor was used to extract the unreacted material and low molecular weight oligomers from the matrix of the copolymers. The extraction solvent used was 2-propanol and the extraction process ran overnight at 90 °C following a procedure described by Luque de Castro and García-Ayuso(71).

5.11. Surface Analysis

The topographical features of the polymers were obtained using a Tescan Vega II LSU scanning electron microscope (Tescan USA, Pennsylvania, United States) operating at 10kV. In order to optimize imaging of the pattern, the stage was slightly tilted approximately 28°.

5.12. Chemical Structure Analysis

The chemical structures of the compounds used were obtained using a Bruker AVANCE 200 MHz nuclear magnetic resonance spectrometer (Bruker Corp., Milton, Canada). The solvent used was deuterated chloroform.

5.13. Mass Determination

The mass spectrum of the oPEG monomer was obtained using a Waters/Micromass Global Q-TOF (Quadrupole-Time of Flight) mass spectrometer. The sample was run in ESI(+ve) mode at 6000 mass resolution.

6. References

1. Nicolson, P. C.; Vogt, J. Soft contact lens polymers: an evolution. *Biomater.* **2001**, *22* (24), 3273-3283.
2. Tuohy, K. M. Contact lens. 2510438, Jun 6, 1950.
3. Wichterle, O.; Lim, D. Hydrophilic gels for biological use. *Nature* **1960**, *185*, 117-118.
4. DeCarle, J. Developing hydrophilic lenses for continuous wearing. *Aust. J. Optom.* **1972**, *55* (9), 343-346.
5. Reuben, M.; Brown, N.; Lobascher, D.; Chaston, J.; Morris, J. Clinical manifestations secondary to soft lens wear. *Br. J. Ophthalmol.* **1976**, *60* (7), 529-530.
6. Schneider, A.; Francius, G.; Obeid, R.; Schwinté, P.; Hemmerlé, J.; Frisch, B.; Schaaf, P.; Voegel, J.; Senger, B.; Picart, C. Polyelectrolyte multilayers with a tunable Young's modulus: influence of film stiffness on cell adhesion. *Langmuir* **2006**, *22* (3), 1193-1200.
7. Discher, D. E.; Janmey, P.; Wang, Y. Tissue cells feel and respond to the stiffness of their substrate. *Science* **2005**, *310* (5751), 1139-1143.
8. Ruoslahti, E.; Pierschbacher, M. D. New perspectives in cell adhesion: RGD and integrins. *Science* **1987**, *238* (4826), 491.
9. Pelham, R. J.; Wang, Y. Cell locomotion and focal adhesions are regulated by substrate flexibility. *Proc. Natl. Acad. Sci. USA* **1997**, *94* (25), 13661-13665.
10. Lichter, J. A.; Thompson, M. T.; Delgadillo, M.; Nishikawa, T.; Rubner, M. F.; Van Vliet, K. J. Substrata mechanical stiffness can regulate adhesion of viable bacteria. *Biomacromol.* **2008**, *9* (6), 1571-1578.
11. Ulery, B. D.; Nair, L. S.; Laurencin, C. T. Biomedical applications of biodegradable polymers. *J. Polym. Sci., Part B: Polym. Phys.* **2011**, *49* (12), 832-864.
12. Kohane, D. S.; Langer, R. Polymeric Biomaterials in Tissue Engineering. *Pediatric Research* **2008**, *63* (5), 487-491.

13. Vert, M. Polymeric biomaterials: Strategies of the past vs. strategies of the future. *Prog. Polym. Sci.* **2007**, *32* (8), 755-761.
14. Ulbricht, M.; Mutuschewski, H.; Oechel, A.; Hicke, H. Photo-induced graft polymerization surface modifications for the preparation of hydrophilic and low-protein-adsorbing ultrafiltration membranes. *J. Membr. Sci.* **1996**, *115* (1), 31-47.
15. George, P. A.; Donose, B. C.; Cooper-White, J. J. Self-assembling polystyrene-block-poly(ethylene oxide) copolymer surface coatings: Resistance to protein and cell adhesion. *Biomater.* **2009**, *30* (13), 2449-2456.
16. Bridgett, M. J.; Davies, M. C. Control of staphylococcal adhesion to polystyrene surfaces by polymer surface modification with surfactants. *Biomater.* **1992**, *13* (7), 411-416.
17. Ikeda, Y. Surface modification of polymers for medical applications. *Biomater.* **1994**, *15* (10), 725-736.
18. Churaev, N. V.; Esipova, N. E.; Hill, R. M.; Sobolev, V. D.; Starov, V. M.; Zorin, Z. M. The superwetting effect of trisiloxane surfactant solutions. *Langmuir* **2001**, *17* (5), 1338-1348.
19. Venzmer, J.; Wilkowski, S. P. Trisiloxane surfactants--mechanism of spreading and wetting. In *Pesticide Formulations and Applications Systems*; Nalewaja, J. D., Goss, G. R., Tann, R. S., Eds.; American Society for Testing and Materials, 1998; Vol. 18.
20. Halverson, J.; Maldarelli, C.; Couzis, A.; Koplik, J. Wetting of hydrophobic substrates by nanodroplets of aqueous trisiloxane and alkyl polyethoxylate surfactant solutions. *Chem. Eng. Sci.* **2009**, *64* (22), 4657-4667.
21. Kanner, B.; Reid, W. G.; Petersen, I. H. Synthesis and properties of siloxane polyether copolymer surfactants. *Ind. Eng. Chem. Prod. Res. Dev.* **1967**, *6* (2), 88-92.
22. Wagner, R.; Wu, Y.; Czichocki, G.; von Berlepsch, H.; Weiland, B.; Rexin, F.; L., P. Silicon-modified surfactants and wetting: I. Synthesis of the single components of Silwet L77 and their spreading performance on a low-energy solid surface. *Appl. Organomet. Chem.* **1999**, *13* (9), 611-620.
23. Svitova, T.; Hoffmann, H.; Hill, R. M. Trisiloxane surfactants: surface/interfacial tension dynamics and spreading on hydrophobic surfaces. *Langmuir* **1996**, *12* (7),

1712-1721.

24. Wagner, R.; Wu, Y.; Czichocki, G.; von Berlepsch, H.; Rexin, F.; Perepelittchenko, L. Silicon-modified surfactants and wetting: II. Temperature-dependent spreading behavior of oligoethylene glycol derivatives of heptmethyltrisiloxane. *Appl. Organomet. Chem.* **1999**, *13* (3), 201-208.
25. Zhu, X.; Miller, W. G.; Scriven, L. E.; Davis, H. T. Superspreading of water-silicone surfactant on hydrophobic surfaces. *Colloids Surf., A* **1994**, *90* (1), 63-78.
26. Karapetsas, G.; Craster, R. C.; Matar, O. K. On surfactant-enhanced spreading and superspreading of liquid drops on solid surfaces. *J. Fluid Mech.* **2011**, *670*, 5-37.
27. Tiberg, F.; Cazabat, A. Spreading of thin films of ordered nonionic surfactants. Origin of the stepped shape of the spreading precursor. *Langmuir* **1994**, *10* (7), 2301-2306.
28. Rafai, S.; Sarker, D.; Bergeron, V.; Meunier, J.; Bonn, D. Superspreading: aqueous surfactant drops spreading on hydrophobic surfaces. *Langmuir* **2002**, *18* (26), 10486-10488.
29. Kumar, N.; Couzis, A.; Maldarelli, C. Measurement of the kinetic rate constants for the adsorption of superspreading trisiloxanes to an air/aqueous interface and the relevance of these measurements to the mechanism of superspreading. *J. Colloid Interface Sci.* **2003**, *267* (2), 272-285.
30. Wang, C. J.; Liu, Z. Q. Foliar uptake of pesticides--Present status and future challenge. *Pestic. Biochem. Physiol.* **2007**, *87* (1), 1-8.
31. Zabkiewicz, J. A.; Gaskin, R. E. In *Adjuvants and Agrochemicals*; Chow, N. P., Grant, C. A., Hinshalwood, A., Sigmundsson, E., Eds.; CRC Press: Boca Raton, Florida, 1989; Vol. 1, p 141.
32. Knoche, M.; Tamura, H.; Bukovax, M. J. Performance and stability of the organosilicon surfactant L-77: effect of pH, concentration, and temperature. *J. Agric. Food Chem.* **1991**, *39* (1), 202-206.
33. Gaskin, R. E.; Kirkwood, R. C. In *Adjuvants and Agrochemicals: Mode of Action and Physiological Activity*; Chow, N. O., Grant, C. A., Hinshalwood, A., Sigmundsson, E., Eds.; CRC Press: Boca Raton, Florida, 1989; Vol. 1, p 129.

34. Young, T. An essay on the cohesion of fluids. *Philos. Trans. R. Soc. London* **1805**, 95, 65-87.
35. Tadmor, R. Line energy and the relationship between advancing, receding, and Young contact angles. *Langmuir* **2004**, 20 (18), 7659-7664.
36. Dahlgren, C.; Sunqvist, T. Phagocytosis and hydrophobicity: a method of calculating contact angles based on the diameter of sessile drops. *J. Immunological Methods* **1981**, 40 (2), 171-179.
37. Skinner, F. K.; Rotenberg, Y.; Neumann, A. W. Contact angle measurements from the contact diameter of sessile drops by means of a modified axisymmetric drop shape analysis. *J. Colloid Interface Sci.* **1989**, 130 (1), 25-34.
38. Chua, D. B.; Ng, H. T.; Li, S. F. Y. Spontaneous formation of complex and ordered structures on oxygen-plasma-treated elastomeric polydimethylsiloxane. *Appl. Phys. Lett.* **2000**, 76 (6), 721-723.
39. Bowden, N.; Huck, W. T. S.; Paul, K. E.; Whitesides, G. M. The controlled formation of ordered, sinuoidal structures by plasma oxidation of an elastomeric polymer. *Appl. Phys. Lett.* **1999**, 75 (17), 2557-2559.
40. Bowden, N.; Brittain, S.; Evans, A. G.; Hutchinson, J. W.; Whitesides, G. M. Spontaneous formation of ordered structures in thin films of metals supported on an elastomeric polymer. *Nature* **1998**, 393 (6681), 146-149.
41. Shao, Y.; Brook, M. A. Structured metal films on silicone elastomers. *J. Mater. Chem.* **2010**, 20 (39), 8548-8556.
42. Ambasta, B. K. Polymers and Polymerization. In *Chemistry for Engineers*; Laxmi Publications Ltd.: New Delhi, 2006; pp 179-232.
43. Gracias, D. H.; Somorjai, G. A. Continuum force microscopy study of the elastic modulus, hardness and friction of polyethylene and polypropylene surfaces. *Macromol.* **1998**, 31 (4), 1269-1276.
44. Park, J. H.; Park, K. D.; Bae, Y. H. PDMS-based polyurethanes with MPEG grafts: synthesis, characterization and platelet adhesion study. *Biomater.* **1999**, 20 (10), 943-953.

45. Glass Transition Temperature for Selected Polymers. In *Handbook of Chemistry and Physics*, 87th ed.; Lide, D. R., Ed.; CRC Press: Boca Raton, Florida, 2006; pp 13.6-13.12.
46. Creton, C. Pressure sensitive adhesives: an introductory course. *MRS Bull.* **2003**, *28* (6), 434-439.
47. Creton, C.; Papon, E. Materials science of adhesives: how to bond things together. *MRS Bull.* **2003**, *28* (6), 419-423.
48. Zosel, A. The effect of fibrillation on the tack of pressure sensitive adhesives. *Int. J. Adhes. Adhes.* **1998**, *18* (4), 265-271.
49. Cowles, R. S.; Cowles, E. A.; McDermott, A. M.; Ramoutar, D. "Inert" Formulation Ingredients with Acitivity: Toxicity of Trisiloxane Surfactant Solutions to Twospotted Spider Mites (Acari: Tetranychidae). *J. Econ. Entomol.* **2000**, *93* (2), 180-188.
50. Salem, I. E. M.; Salem, A. E. M. Surfactants including household detergents for controlling the black bean aphid, *Aphis craccivora* Koch (Hom.: Aphididae). *Meded. Fac. Landbouww. Rijsuniv. Gent* **1983**, *48* (2), 225-233.
51. Dentener, P. R.; Peetz, S. M. Postharvest control of diapausing twospotted sider mite, *Tetranychus urticae* Koch, on fruit. I. Comparison of insecticidal soaps and spray adjuvants. *Proc. NZ Plant Protection Conf.* **1992**, *45*, 116-120.
52. Imai, T.; Tsuchiya, S.; Fujimori, T. Surface tension-dependent surfactant toxicity on the green peach aphid, *Myzus persicae* (Sulzer) (Hemiptera). *Appl. Entomol. Zool.* **1994**, *29* (3), 389-393.
53. Imai, T.; Tsuchiya, S.; Morita, K.; Fujimori, T. Aphicidal effects of Silwet L-77, organosilicone nonionic surfactant. *Appl. Entomol. Zool.* **1995**, *30* (2), 380-382.
54. Chandler, L. D. Effect of surfactants on beet armyworm and fall armyworm larvae. *Arthr. Manag. Tests* **1995**, *20*, 353-354.
55. Purcell, M. F.; Schroeder, W. J. Effects of Silwet L-77 and diazinon on three tephritid fruit flies (Diptera: Tephritidae) and associated endoparasitoids. *J. Econ. Entomol.* **1996**, *89* (6), 1566-1570.

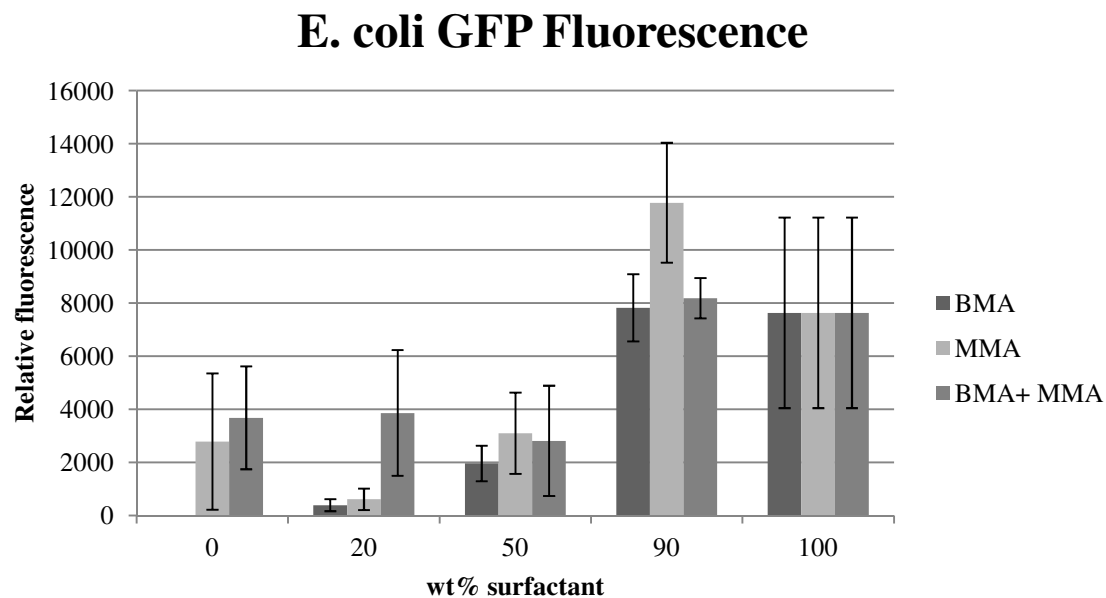
56. Wood, B. W.; Tedders, W. L.; Taylor, J. Control of pecan aphids with an organosilicone surfactant. *Hort Science* **1997**, *32* (6), 1074-1076.
57. Shapiro, J.; Schroeder, W. J.; Stansly, P. A. Bioassay and efficacy of *Bacillus thuringiensis* and an organosilicone surfactant against the citrus leafminer (Lepidoptera: Phylloncnistidae). *Florida Entomol.* **1998**, *81* (2), 201-210.
58. Banks, A. R.; Fibiger, R. F.; Jones, T. A convenient synthesis of methacrylates. *J. Org. Chem.* **1977**, *42* (24), 3965-3966.
59. Chen, W.; Shull, K. R. Hydrophilic surface coatings from acrylic block copolymers. *Macromol.* **1999**, *32* (19), 6298-6306.
60. Chen, W.; Shull, K. R.; Papatheodorou, T.; Styrkas, D. A.; Keddie, J. L. Equilibrium swelling of hydrophilic polyacrylates in humid environments. *Macromol.* **1999**, *32* (1), 136-144.
61. Bartzoka, V.; McDermott, M. R. . B. M. A. Protein silicone interactions. *Biomater.* **2002**, *23* (3), 1797-1808.
62. Anderson, J. M.; Ziats, N. P.; Azeez, A.; Brunstedt, M. R.; Stack, S.; Bonfield, T. L. Protein adsorption and macrophage activation on polydimethylsiloxane and silicone rubber. *J. Biomater. Sci., Polym. Ed.* **1996**, *7* (2), 159-169.
63. Chen, H.; Brook, M. A.; Chen, Y.; Sheardown, H. Surface properties of PEO-silicone composites: reducing protein adsorption. *J. Biomater. Sci., Polym. Ed.* **2005**, *16* (4), 531-548.
64. Chen, H.; Zhang, Z.; Chen, Y.; Brook, M. A.; Sheardown, H. Protein repellent silicone surfaces by covalent immobilization of poly(ethylene oxide). *Biomater.* **2005**, *26* (15), 2391-2399.
65. Kingshott, P.; Thissen, H.; Griesser, H. J. Effects of cloud-point grafting, chain length, and density of PEG layers on competitive adsorption of ocular proteins. *Biomater.* **2002**, *23* (9), 2043-2056.
66. Szleifer, I. Polymers and proteins: interactions at interfaces. *Curr. Opin. Solid State Mater. Sci.* **1997**, *2* (3), 337-344.

67. Auroy, P.; Auvray, L.; Leger, L. Characterization of the brush regime for grafted polymer layers at the solid-liquid interface. *Phys. Rev. Lett.* **1991**, *66* (6), 719-722.
68. Snow, S. A.; Fenton, W. N.; Owen, M. J. Synthesis and Characterization of Zwitterionic Silicone Sulfobetaine Surfactants. *Langmuir* **1990**, *6* (2), 385-391.
69. Snow, S. A.; Fenton, W. N.; Owen, M. J. Zwitterionic organofunctional siloxanes as aqueous surfactants: synthesis and characterization of betaine functional siloxanes and their comparison to sulfobetaine functional siloxanes. *Langmuir* **1991**, *7* (5), 868-871.
70. Fullard, R. J.; Tucker, D. L. Changes in human tear protein levels with progressively increasing stimulus. *Invest. Ophthalmol. Vis. Sci.* **1991**, *32* (8), 2290-2301.
71. Luque de Castro, M. D.; García-Ayuso, L. E. Soxhlet extraction of solid materials: an outdated technique with a promising innovative future. *Anal. Chim. Acta* **1998**, *369* (1-2), 1-10.
72. Knoche, M. Organosilicone surfactant performance in agricultural spray application: a review. *Weed Res.* **1994**, *34* (3), 221-239.
73. Hill, R. M. Comparison of the Liquid Crystal Phase Behavior of Four Trisiloxane Superwetter Surfactants. *Langmuir* **1994**, *10* (6), 1724-1734.
74. Hill, R. M. Siloxane Surfactants. In *Silicone Surfactants*; Hill, R. M., Ed.; Marcel Dekker, Inc.: New York, 1999; pp 1-48.
75. Hoffmann, H.; Ulbricht, W. Surface Activity and Aggregation Behavior of Siloxane Surfactants. In *Silicone Surfactants*; Hill, R. M., Ed.; Marcel Dekker, Inc.: New York, 1999; pp 98-136.

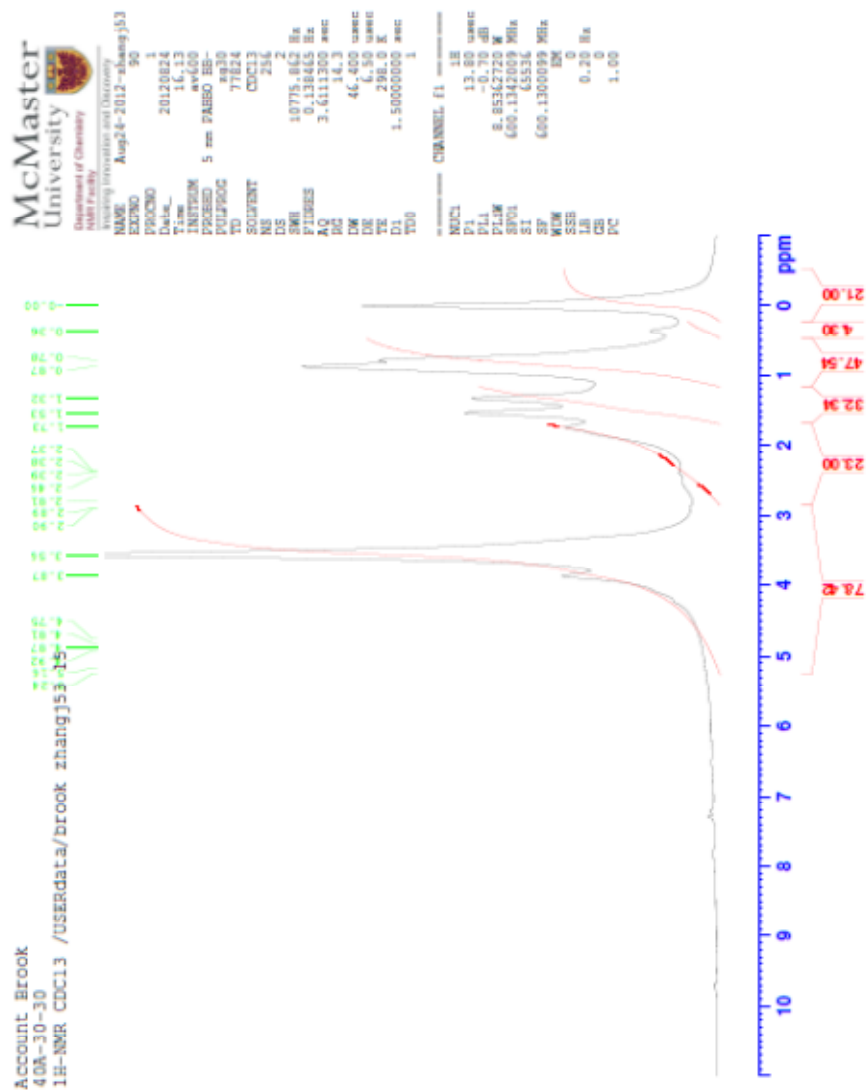
7. Appendix

7.1. E. coli GFP Fluorescence

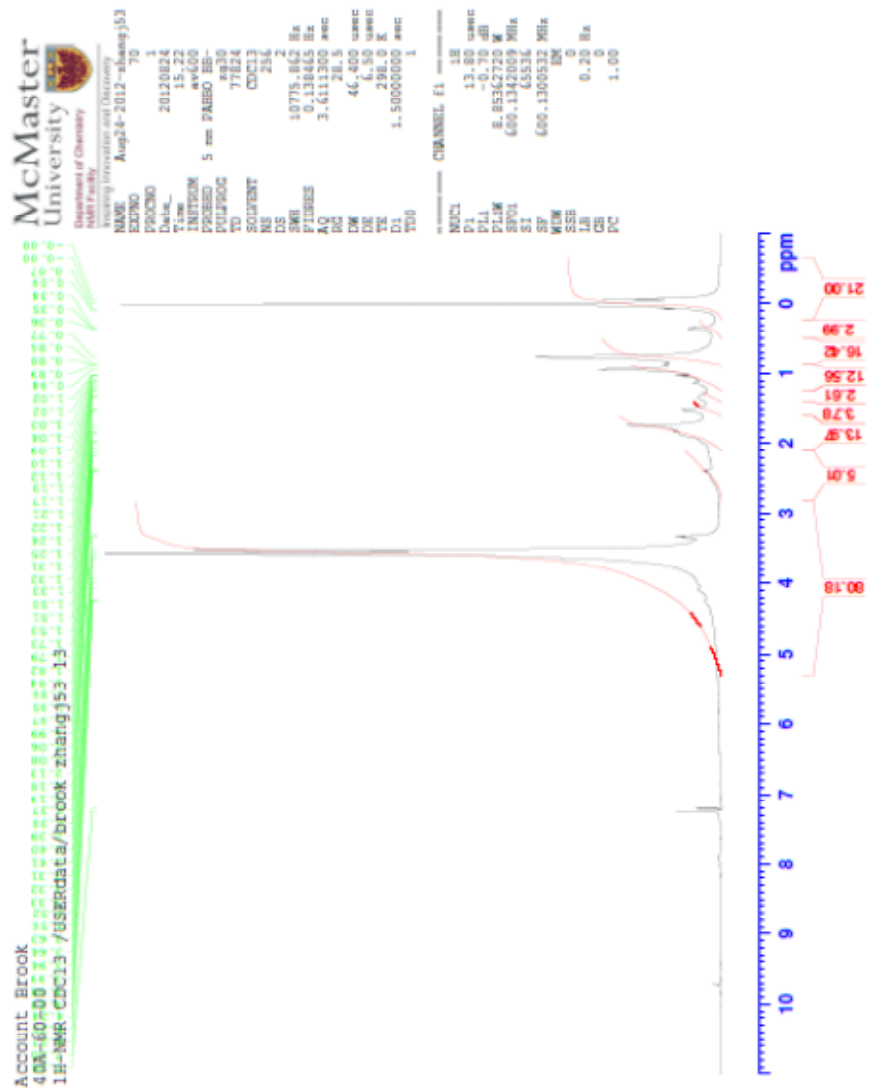
Disclaimer: This bacterial fluorescence study was completed by Madiha Khan. The details of these bacterial studies will be undertaken in future works.



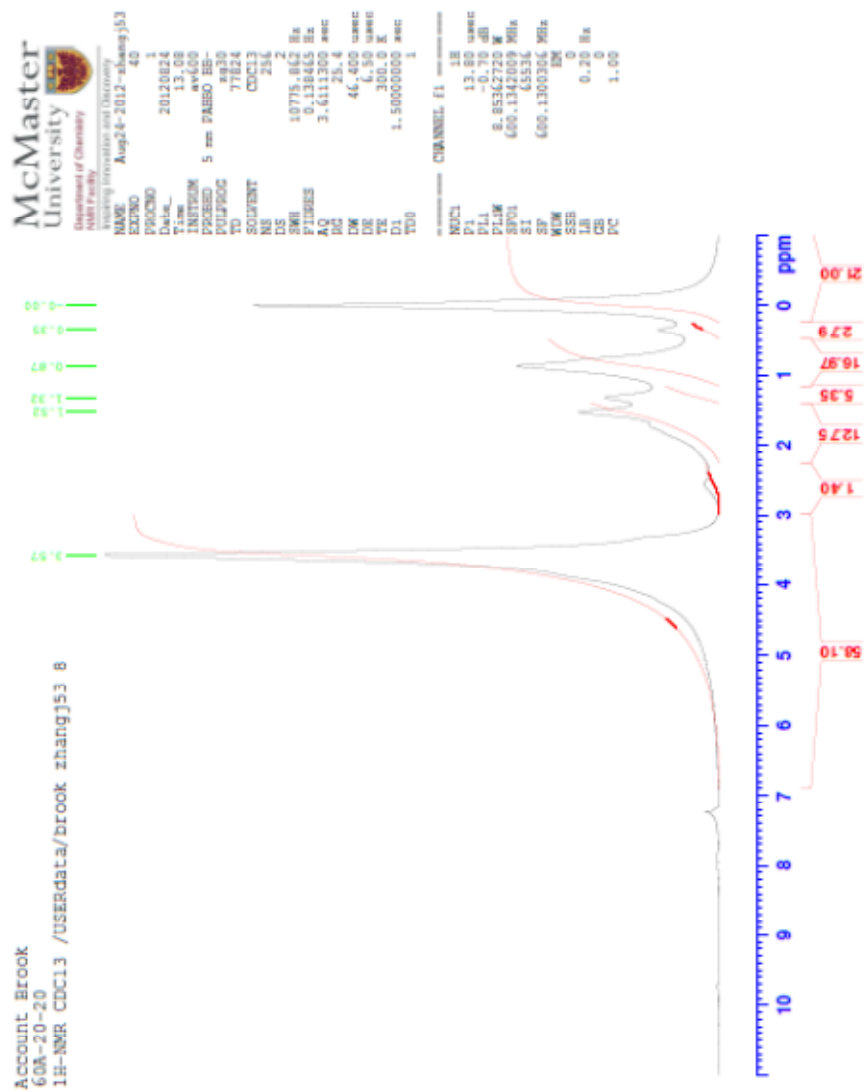
7.2.2. 40-30-30



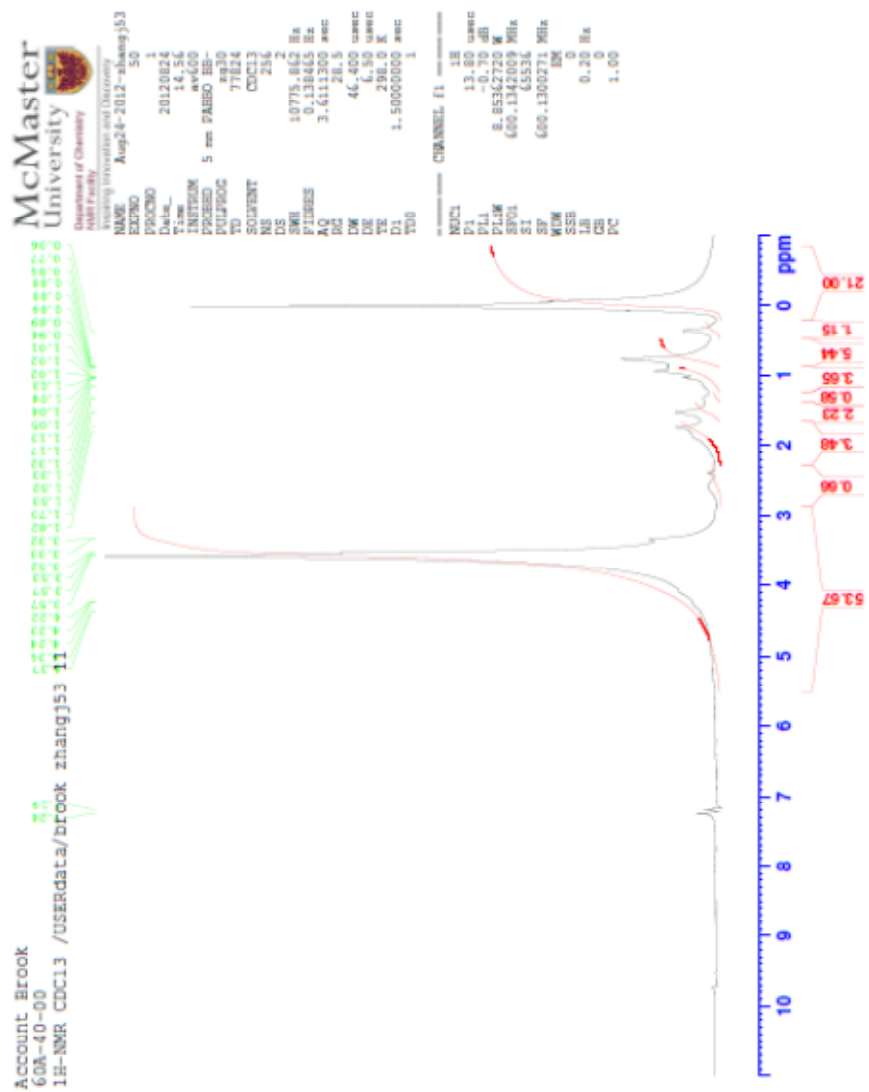
7.2.3. 40-60-00



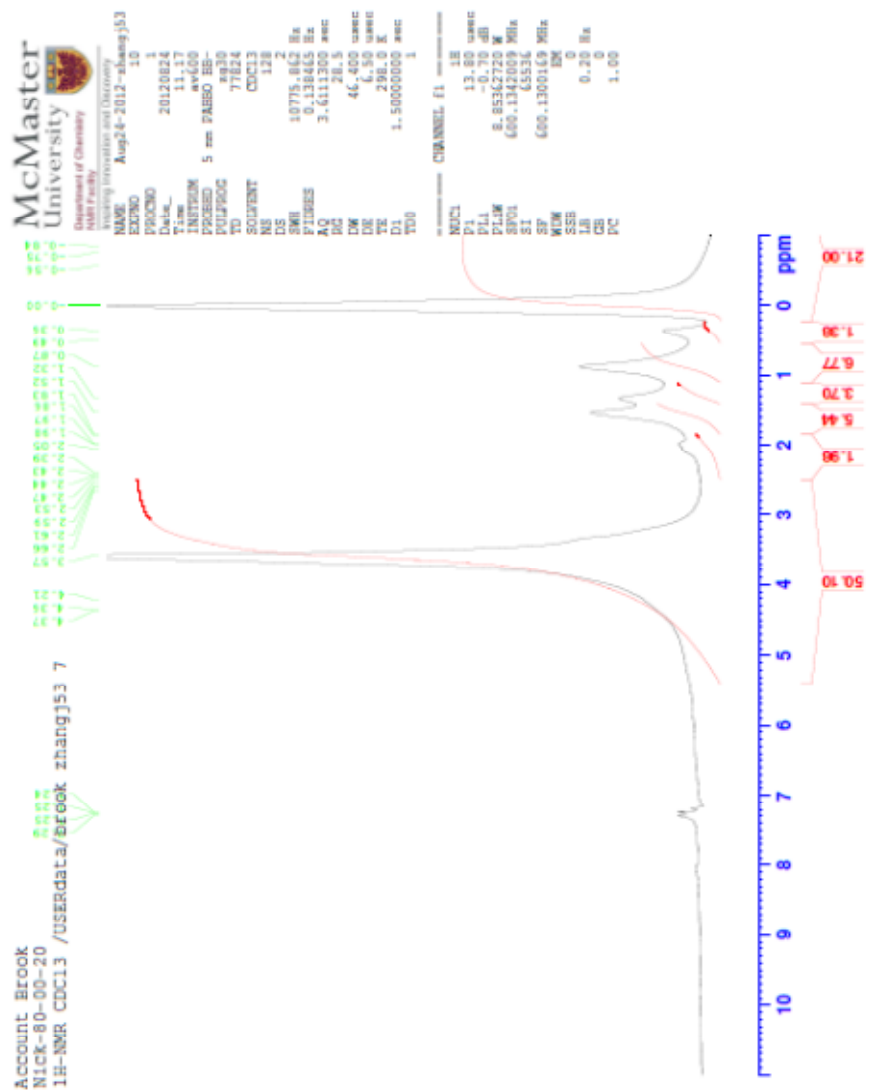
7.2.5. 60-20-20



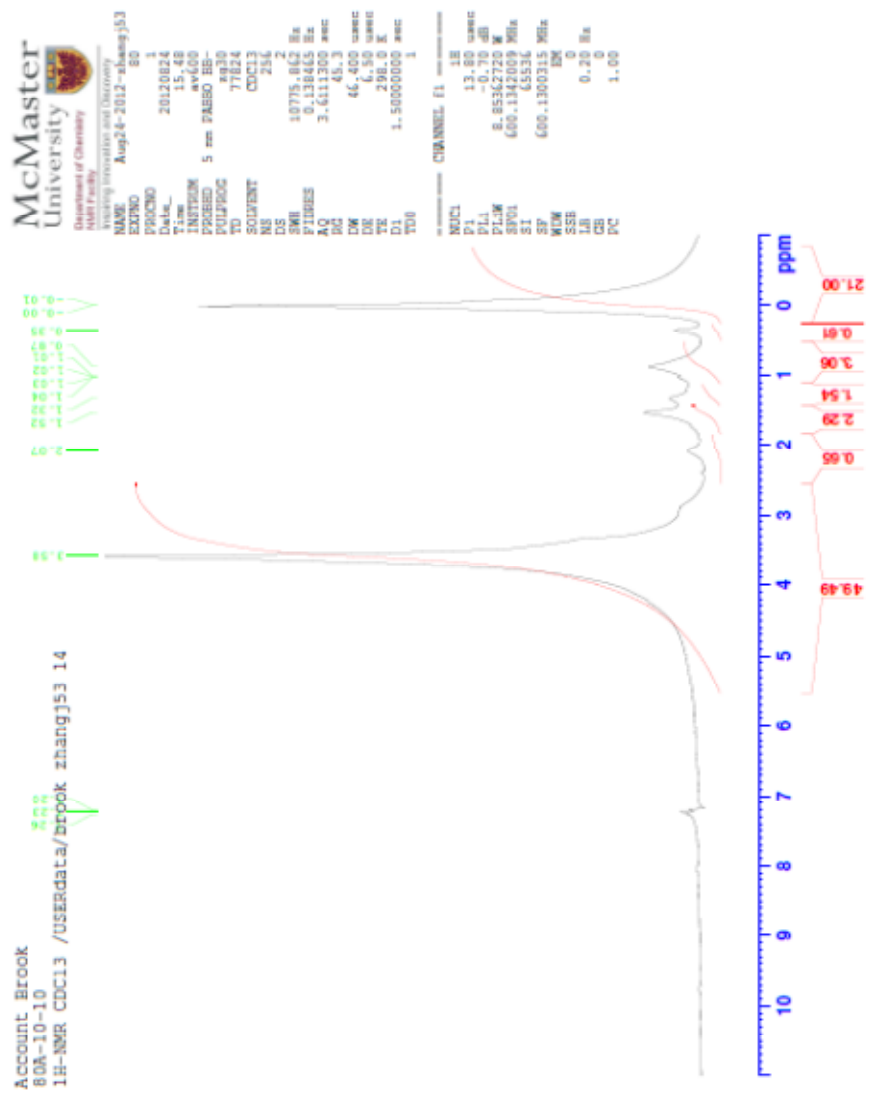
7.2.6. 60-40-00



7.2.7. 80-00-20



7.2.8. 80-10-10



7.2.9. 80-20-00

